Graz University of Technology

Institute of Biomechanics
Center of Biomedical Engineering
Kronesgasse 5-I
8010 Graz, Austria

Master's Thesis

Macroscopic stress and strain generation in electrically stimulated human ventricular myocardium

to achieve the degree of
Master of Science

Author: Manuel Huber, BSc
Supervisor: Gerhard Sommer, PhD

Head of Institute: Professor Gerhard A. Holzapfel, PhD

August 24, 2015

Contents

List of Figures

List of Tables

Abstract

Cardiovascular diseases are the leading cause of death in Austria and a growing epidemic, primarily in industrialized countries. While extensive research on the passive mechanical properties of human myocardial tissue has already been done, information about the active electrophysiologial behavior are limited, particularly due to the absence of simple but representative experimental setups. However, active data is essential in order to get a holistically understanding of structure and function from a biomechanical point of view. The determination of the mechanical behavior of the myocardium is also the central problem in finite element simulation (FEM) to study the heart contraction and excitation propagation and to take a step forward in the development of an artificial heart. For the first time, the active mechanical characteristics of myocardial tissue was investigated at the Technical University of Graz. Therefore, the goal of this Master's thesis was to establish an isometric experimental setup utilizing an uniaxial tensile testing machine. Furthermore, an applicable measurement report had to be included, allowing measurement of the occurring stress and strain data in heart slices during a contraction. The whole study must be considered as foundational research.

Since only specimens of four hearts were tested, representative statements are difficult to make. Notwithstanding, certain trends could be found. Although the received hearts were classified as non-failing, a negative stress/force-frequency relationship was observed, indicating pathological tissue. The force-frequency relationship is a significant intrinsic regulatory mechanism of heart contraction. Additionally, it was shown that the length-dependent activation, one of the most important aspects of the Frank-Starling mechanism, is still existing in human myocardial slices. For the first time, according to the knowledge of the author, the two-dimensional strain on the surface of the specimen was measured and evaluated by the method of Digital Image Correlation. In addition, the time behavior of individual contractions for both stress and strain was analyzed.

In summary, an experimental setup could be established. In further research, thinner human myocardial slices cut in muscle fiber direction should be tested in order to maintain sufficient nutrient and oxygen supply through to the core of the specimens. Therefore, more representative findings could be received to extend the material parameters of the Institute of Biomechanics' FEM heart model by active mechanical properties.

Zusammenfassung

Kardiovaskuläre Erkrankungen stellen eine wachsende Epidemie in Industrieländern dar und sind gleichzeitig die häufigste Todesursache in Österreich. Während die passiven mechanischen Eigenschaften des menschlichen Myokards bereits gut erforscht sind, sind Informationen über das aktive elektrophysiologische Verhalten in der Literatur kaum zu finden, was vor allem auf das Fehlen eines einfachen aber repräsentativen experimentellen Setups zurückzuführen ist. Daten über die aktiven Eigenschaften sind jedoch notwendig um die Struktur und die Funktion aus biomechanischer Sicht ganzheitlich verstehen zu können. Die Bestimmung des mechanischen Verhaltens des Myokards ist auch das zentrale Problem in der Finite-Elemente-Methode Simulation (FEM), um die Herzkontraktion und die Erregungsausbreitung studieren zu können und in der Entwicklung von künstlichen Herzen Fortschritte zu erzielen. Da am Institut für Biomechanik der Technischen Universität Graz noch nie zuvor die aktiven mechanischen Eigenschaften von Herzgewebe bestimmt wurden, war das Ziel dieser Masterarbeit ein isometrisches experimentelles Setup auf Basis einer uniaxialen Zugprüfmaschine inkl. eines geeigneten Messprotokolls zu etablieren, mit welchem die auftretenden Spannungen und Dehnungen von Herzscheiben während der Kontraktion gemessen werden konnten. Die gesamte Studie muss als Grundlagenforschung angesehen werden.

Da nur vier Herzen getestet wurden sind repräsentative Aussagen schwierig zu treffen, es zeichneten sich jedoch eindeutige Trends ab. Obwohl die empfangenen Herzen als gesund eingestuft wurden, zeigten sie eine negative Kraft-Frequenz Beziehung welche auf pathologisches Gewebe hindeutet. Diese Kraft-Frequenz Beziehung ist ein wichtiger intrinsischer Regulierungsmechanismus der Herzkontraktion. Weiters konnte gezeigt werden, dass die längenabhängige Aktivierung, ein wichtiger Bestandteil des Frank-Starling Mechanismus, in den getesteten Proben aufrecht erhalten blieb. Dem Wissen des Autors zufolge, wurde zum ersten Mal die zweidimensionale Dehnung während des Kontraktionszyklus gemessen und mit der Methode der Digitalen Image Correlation ausgewertet. Außerdem wurde das Zeitverhalten der einzelnen Kontraktionen sowohl für die Spannung als auch für die Dehnung analysiert.

Zusammengefasst kann gesagt werden, dass ein experimentelles Setup etabliert werden konnte. In zukünftigen Studien sollten die Proben dünner und immer in Muskelfaserrichtung geschnitten werden um eine ausreichende Sauerstoff- und Nährstoffversorgung bis zum Kern der Proben garantieren zu können und um repräsentative Daten zu liefern, mit welchem das FEM Modell des Institutes für Biomechanik um die aktiven mechanischen Eigenschaften erweitert werden kann.

Acknowledgment

First and foremost, I would like to express my gratitude to my supervisor Dr. Gerhard Sommer for the continuous support and useful discussion throughout the learning process of this Master's thesis. Furthermore, I would like to thank the head of the Institute of Biomechanics Prof. Gerhard A. Holzapfel for having the opportunity to work in the laboratory in order to get the experimental data.
I would like to thank Dr. Karin Hammer and Prof. Frank Heinzel of the Division of Cardiology, Medical University of Graz, for their inspiring discussion at the beginning of this work. I would also like to thank Bakk. Thomas Rau and Georg Pratl of the Division of Cardiology, Medical University of Graz, for their good communication and coordination in the delivering process of the hearts. I wish to thank Dr. Christian Viertler of the Institute of Pathology, Medical University of Graz, for the histological examination of the specimens. Furthermore, I am grateful to Dr. Sae-Il Murtada for the helpful comments on the interpretation and preparation of the measurement data.
Thanks also goes to those who provided equipment to arrange the experimental task: Dr. Michaela Andrä of the Division of Transplantation Surgery, Medical University of Graz, for allowing me to mix the Tyrode's solution, Prof. Gunter Winkler of the Institute for Electronics, Graz University of Technology, for manufacturing the Pt-micro-electrode and lending the function generator, Ing. Friedrich Lazar of the Institute of Hydraulic Engineering and Water Resources Management, Graz University of Technology, for manufacturing the plexiglass container and the heating coil, and Prof. Jörg Schröttner of the Institute of Health Care Engineering, Graz University of Technology, for lending the gas valve.
Last but not least, my deepest gratitude goes to my family, especially to my parents Brigitte and Hubert, for their unflagging love, continuous and unconditional support throughout my life and my studies.

1 Introduction

The task of this Master's thesis is to examine the macroscopic stress and strain generation in electrically stimulated human ventricular myocardium. For the first time mechanical properties of living human myocardium were tested at the Institute of Biomechanics, Graz University of Technology. For this reason, a new experimental setup and measurement report had to be established utilizing an uniaxial tensile testing machine to perform isometric contraction investigations. Since human tissue cells can only survive for a limited period of time, logistics became a challenge. The main focus was placed on the stress/force-frequency relationship of the myocardial tissue including the evaluation of timing parameters (twitch-time and time-to-peak) at various pre-stretches. For the first time, according to the knowledge of the author, the two-dimensional strain of the human myocardial tissue was measured. To perform control experiments, stimulation parameters (pulse width and stimulation voltage) were altered. Thickness and width of the tissue specimens were measured. For any additional investigation, the tested specimens were placed in formaldehyde, e.g., for the investigation of the fiber direction.
The determination of the mechanical properties of the human ventricular myocardium is a central problem in the Finite Element Method (FEM) analysis of the heart. The FEM analysis, however is essential for the construction of virtual living hearts and studying their mechanical functionality and behavior. The FEM simulation is, for instance, able to give information about the myocardial contraction, the excitation propagation, and the development of an artificial heart. Huge amount of data of cardiac motion can be generated from FEM, particularly information about stress and strain, the two key determinants of many cardiac physiological and pathophysiological processes (Hassan et al. (2012)). Cardiac infarction, cardiac adiposis, cardiac dysfunction, and cardiac myopathy influence the myocardial heart structure and seem to lead to a change of mechanical properties of the heart (Sommer et al. (2012)). The passive mechanical properties (determination using mostly uni- and biaxial tensile tests and triaxial shear tests) are good initial values to start running the simulation for heart biomechanics. In order to get optimized results the material parameters of the constitutive framework have to be adjusted and extended, e.g., by the active mechanical properties of the heart or the residual stresses. Figure 1.1 shows the fundamental requirements in order to be able to run a FEM heart simulation. The results of this Master's thesis should extend the material parameters of the Institute of Biomechanics' FEM heart model, needed for more accurate bio-simulations of the active mechanical properties of the human ventricular myocardium. The conducted experiments are intended as basis for future research in this field (Hassan et al. (2012)).
Since heart transplantation has become a routine surgical intervention, laboratories have

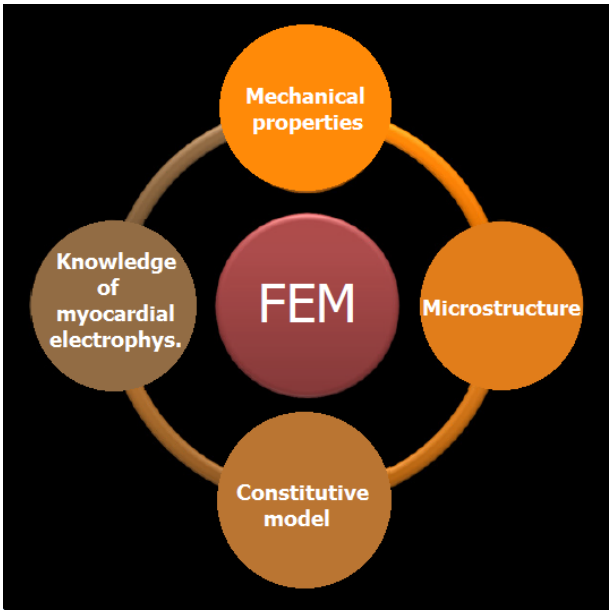

Figure 1.1: Fundamental requirements for FEM heart simulation (Sommer et al. (2012))

the opportunity to get human heart pieces for experimental research under defined ethics instructions. Historically at the beginning, the function of the heart as a pump had been explored. Thereby, the focus was set on the determination of the intravascular and intracardiac pressures, flows, and their derivatives (Sonnenblick et al. (1965)). During the last few decades, the skeletal muscles were further investigated in order to get an understanding of the mechanical behavior and the energy consumption and supply of the muscle tissue (see Sonnenblick et al. (1965)). In the 1960s, the first experiments were performed on isolated parts of the heart muscle (see Sonnenblick et al. (1965)). Attention was paid to the examination of the ventricle in terms of its properties as a muscle (Sonnenblick et al. (1965), Holubarsch et al. (1998)).
Although intensive research for a better understanding in the mechanism of heart arrhythmia and heart diseases with animal myocardium has been conducted, experiments with human myocardium are very rare in literature. This is not only because of the difficulties in getting human heart tissue but also due to the absence of simple experimental testing methods for human myocardial specimens. However, there are major differences in the molecular and cellular level of myocardial tissue between humans and animals, causing the data from such mammalian test systems to be of limited relevance for the human situation. The ideal experiment should fulfill the following requirements (Camelliti et al. (2011)):

1. high representative
2. obtain the original structure, function, and metabolism
3. adequate oxygenation of the tissue

These requirements are essential to perform investigations on the molecular, sub-cellular, cellular, and multicellular level which are integral components of congestive heart failure diseases. Cardiovascular diseases are a growing epidemic, primarily in industrialised countries. The five year mortality of heart failure diseases converges 50 percent. Examination of the human myocardium under *in vitro* conditions seems to be a promising approach in understanding the consequences of a cardiac defect. Since the left-ventricular dysfunction is the most common disease of human heart failure, the left ventricular myocardium is the focal point for *in vitro* investigation (Mulieri et al. (1989), Camelliti et al. (2011), Brandenburger et al. (2012), Moussavi-Harami et al. (2015)).
To date, several experimental methods are available to examine human heart tissue: enzymatically isolated myocytes, intact regions of the myocardium, Langendorff-perfused hearts, *in situ* observations, and myocardial slices. The lack of multicellular and intracellullar connections makes enzymatically isolated myocytes (see Camelliti et al. (2011)) unusable for investigation of multicellular effects such as pharmacological interaction or heart excitation propagation. Aside from that, it is rather difficult to isolate viable myocytes. Still, a large number of myocytes can be examined by a single heart, and therefore a large number of measurements can be made. An alternative approach is the extraction of intact regions of the human heart (see Camelliti et al. (2011)) such as trabeculae, papillary muscle, or ventricular wedges. Trabeculae and papillary muscle retain the natural multicellular structure but are restricted to the endocardial part of the heart. Ventricular wedges require complex perfusion methods to ensure the viability of the tissue. Studies on the entire heart, called Langendorff-perfused heart studies, are extremely rare in literature (see Camelliti et al. (2011)). This kind of examination is rather expensive but at the same time allows approximate *in vivo* conditions. *In situ* observations provide realistic and relevant measurements of cardiac function but hardly any information about the inner heart mechanism (Camelliti et al. (2011)).
A new approach, which was tested for the first time on a rodent heart, is to cut thin slices of living cardiac tissue. Heart slices combine the advantages of entire organs and isolated tissue cells. Thereby, the relevant structures and functional characteristics are preserved and non-enzymatic digestion is carried out. Furthermore, a viability of several hours can be reached *in vitro* and no choice of specific heart cells during the selection process is required. This promising technique was recently applied to two fetal hearts (see Camelliti et al. (2011)). Despite the above mentioned advantages, human heart slices are less often used than slices of other organs because of a set of complications in handling human myocardium. Human tissue slices of several other organs (see Bussek et al. (2009)) e.g., brain, kidney, liver, lung, or pancreas are already being established for standard biochemical and electrophysiological studies (Bussek et al. (2009), Camelliti et al. (2011)).
To date, the potential and feasibility of human myocardial tissue slices as a tool of cardiac research can not be anticipated. Therefore, the aim of this Master's thesis is the systematical determination of the active mechanical behavior of human heart slices. Only little *in vitro* data of the active mechanical properties of human heart strips is available in literature. Studies on the stress/force-frequency relationship of the human papillary muscle, and the

failing and non-failing parts of the human ventricular heart wall could be found (Mulieri et al. (1989), Mulieri et al. (1992), Schwinger et al. (1993), Schwinger et al. (1997), Bavendiek et al. (1998), Holubarsch et al. (1998), Brixius et al. (2001), Brandenburger et al. (2012), Moussavi-Harami et al. (2015)). With its ability to adapt the cardiac pump function to various altering hemodynamics of the body, the force-frequency relationship, in common with the Frank-Starling mechanism, is of great importance to the adjustment of the mechanical performance of the heart. This relationship was first observed as an important control system by Bowditch (1871) who noted that "the interval between a contraction of the heart and the proceeding beat is of such importance for the strength of the contraction that the study of this effect is a prime necessity" (Shiels et al. (2002), Endoh (2004)). Data of the intracellular and extracellular action potential and the propagation velocity measured with multi-electrode arrays on heart tissue are rare in literature (Bussek et al. (2009), Camelliti et al. (2011), Bussek et al. (2012)). Cross-bridge kinetics studies (Hasenfuss et al. (1991), Ruf et al. (1998)) and a huge number of pharmacology intervened studies (Schwinger et al. (1993), Holubarsch et al. (1998), Bussek et al. (2009), Camelliti et al. (2011), Bussek et al. (2012)) using human cardiac tissue slices are available in literature. Yet papers on the strain of rectangular human myocardial slices are very rare. Only one paper could be found in which the one-dimensional isometric contraction shortening of left ventricular tissue slices was measured (Holubarsch et al. (1998)). A number of strain modelling papers of the left ventricle are available in literature (Hu et al. (2003), Phatak et al. (2009)). Two-dimensional strain measurement publications of cardiac tissue slices could not be found. In addition, it should be mentioned that the slice thickness is less than 500 μm in almost all published heart studies, contrary to the threefold to fourfold thicker slices used in this study.

This Master's thesis has the following structure: at the beginning, key facts which are essential to set up the experimental procedure about the human heart will be given. Afterwards, the methods which were used will be explained. This includes the way of the human heart from the explant, to the dissect table in the laboratory, and finally to the uniaxial tensile testing machine and additional information about transport and nutrient solutions. Information about the experimental setup and the general testing procedure will be given. In the third section the experimental measured results will be listed. The main focus is placed on the stress/force-frequency relationship and the two-dimensional strain of the tissue slices. Then, time parameters (twitch-time and time-to-peak), histological report, and performed control experiments data will be listed and evaluated with the help of statistical methods. The fourth section contains the discussion. In this section the experimentally measured results and the derived conclusions will be discussed whereat the focus is placed on the stress/force-frequency relationship and the strain data. The chapter concludes with occurring limitations, open problems and an outlook. This Master's thesis will be completed with the conclusion in which the most important results will be summarized.

1.1 Human heart

In this section general information about the characteristics of biological tissue will be given. Afterwards, the anatomy and the excitation-contraction coupling of the human heart will be described.

1.1.1 Characteristics of biological tissue

Living biological tissue shows characteristics different than normal engineering material such as steel or aluminum. For example, the aging, the repair mechanisms as well as the ability to adapt to various conditions make biological tissue more complex. Nevertheless, in experimental tasks biological tissue will be treated as engineering material under defined environmental conditions. Most biological materials consist of several components - each of them with different mechanical behavior (known as inhomogeneous behavior). Anisotropy also plays an important role. In anisotropic tissues, the mechanical properties depend on the direction of an applied force (fibers have preferred directions). In addition, almost all biological materials exhibit a viscoelastic behavior and will be modelled as incompressible. As a result, it is much more difficult to describe the mechanical properties of living human tissue than that of engineering material (Oezkaya and Nordin (1999)).
In general, the determination of biomechanical properties of the human cardiac muscle is more demanding than that of a skeletal muscle, particularly because of the heart muscle refractory period and the lack of an ideal cardiac test specimen. It should be noted that the human heart possesses residual stresses. Moreover, a distinction between the active and passive mechanical properties of the ventricular myocardium is necessary. The passive mechanical behavior of the myocardium is well known. In uniaxial cyclic tests, resting human heart myocardium shows similar characteristics to normal soft biological tissue: non-linear stress-strain diagram with a small but significant hysteresis. The main components which determine the passive mechanical behavior are the two proteins collagen and elastin. Collagen fibers possess a high tensile strength, strict organization of the fibers (anisotropic behavior), and poor resistance to compression. Collagen is found in all soft tissues and takes the load when the force is increased. Elastin has a rubber chain property, shows no strict organization (isotropic behavior), is highly extensible, and shows no plastic deformation before failures occur. Furthermore, the load and unload curve of elastin shows hardly any hysteresis (Oezkaya and Nordin (1999), Holzapfel and Unterberger (2010)).
Compared to the passive properties, data concerning the active mechanical properties of the human myocardium is rare in literature, mainly because of two reasons: it is problematic to get living human myocardium to test the active behavior (huge data of tested animal tissue is available and it is easier to test than the 'softer' human tissue) and to keep the tissue alive (in particular samples with a thickness of about 1 mm or more).

1.1.2 Heart anatomy

The healthy human heart is a hollow, muscular organ with the size of a fist and a weight of about 250 to 400 gram. The longitudinal axis of the heart is obliquely oriented and runs from the right back top to the left front down. It is surrounded by a serous layer that is called the two-layered heart sac (pericardium). The pericardium contains a fluid which facilitates the sliding movement during contraction (systole) and relaxation (diastole) of the heart muscle. The heart is composed almost symmetrically and is divided into a left and a right half by the septum. Initially the blood flows to the right heart. Then it rushes through the pulmonary artery into the lungs to absorb oxygen. The oxygenated blood flows through the pulmonary veins to the left heart. The blood leaves the left heart via the aorta and flows to all organs of the human body.
The heart consists of four pumping chambers: right and left atria and ventricles. The two coronary arteries are located between the atria and ventricles. Their purpose is to supply the heart muscle with nutrients. The task of the atria is to collect the blood which returns from the systemic (right atrium) and the pulmonary circulation (left atrium). Via the two atrioventricular valves (right heart: tricuspid valve, left heart: mitral valve) the blood flows from the atria to the ventricle. The task of the ventricles is to pump the blood through the pulmonary artery into the lung (right ventricle, via the pulmonary valve) and through the aorta into the organs of the body (left ventricle, via the aortic valve). The left ventricle has an ellipsoid form with a physiologically high pressure of about 15 kPa (120 mmHg). A low pressure domain of about 2 kPa (15 mmHg) and a crescent shape characterizes the right ventricle. Due to the physiologically high pressure domain of the left heart, the myocardium of the left ventricle is thicker (about 15 mm) than that of the right ventricle (about 5 mm). Figure 1.2 shows a schematic composition of the human heart.
The human heart wall is arranged in a layered structure in which the direction of the fibers is shifting through the location (Speckmann and Wittkowski (2004)). The heart wall consists of three layers:

- inner layer: endocardium
- middle layer: myocardium
- outer layer: epicardium

The epicardium is separated from the pericardium by a sliding gap which is filled with serous liquid. The coronary arteries supply the myocardium and the epicardium with nutrients. The endocardium lines the inner space of the heart and forms the heart valves. It consists of the endothelium and connective tissue (collagen and elastin) and is about 0.5 mm to 1 mm thick. The epicardium is a thin membrane which contains collagen and elastic fibers. The most important and also thickest layer is the strong myocardium with the cardiac muscle cell as the predominant component. The myocardium acts as the pumping tissue and consists of highly organized striated muscle fibers. These fibers are branched (connected by intercalated disks) and together they form a dense network including lots of blood vessels. Every single heart muscle cell (called cardiomyocytes) is able to contract. The excitation is forwarded to all the cells if a stimulus is high enough to initiate a

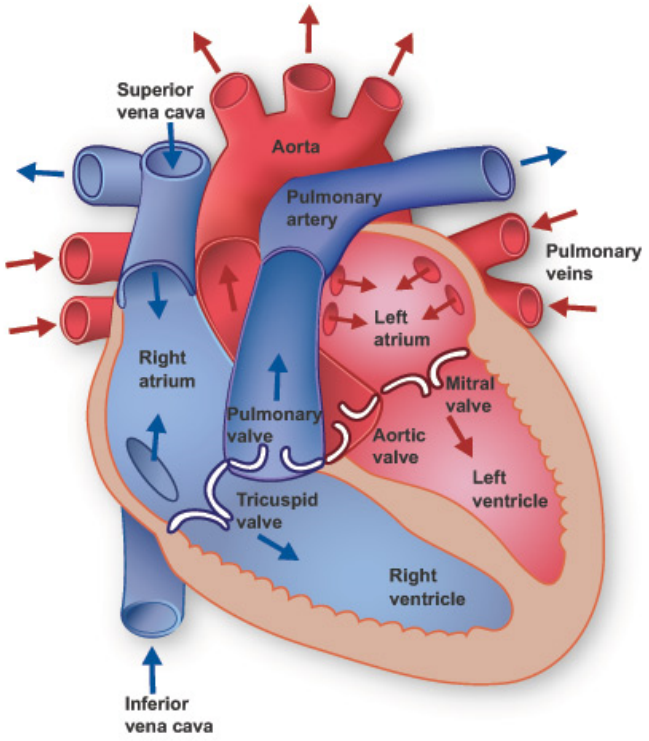

Figure 1.2: Schematic composition of the human heart (taken from http://www.texasheartinstitute.org/HIC/Anatomy/anatomy2.cfm)

depolarization ("The heart could be seen as one large, single cell"). Figure 1.3 shows the structure of the human heart wall. The healthy adult human heart beats with a frequency of about 70 bpm (beats per minute). With every heart beat about 70 ml blood will be ejected in the aorta (stroke volume). This results in a cardiac output of nearly 5 liter per minute which corresponds approximately to the total blood volume of the body (Speckmann and Wittkowski (2004)).

The ejection fraction (*EF*) is one of the most important parameters for the evaluation of the cardiac function. It is defined as the ratio of the stroke volume (*SV*) to the total blood volume of the ventricle, also known as end-diastolic volume (*EDV*, typical value of about 120 ml) and can be seen in Eq. 1.1:

$$EF(\%) = \frac{SV}{EDV} \cdot 100\ . \tag{1.1}$$

To calculate the stroke volume Eq. 1.2 is required, where *ESV* is the end-systolic volume (typical value of about 50 ml):

$$SV = EDV - ESV\ . \tag{1.2}$$

The *EF* is usually measured by echocardiography. In the healthy human heart the *EF* should be higher than or equal to 55% (Solomon (2007)).

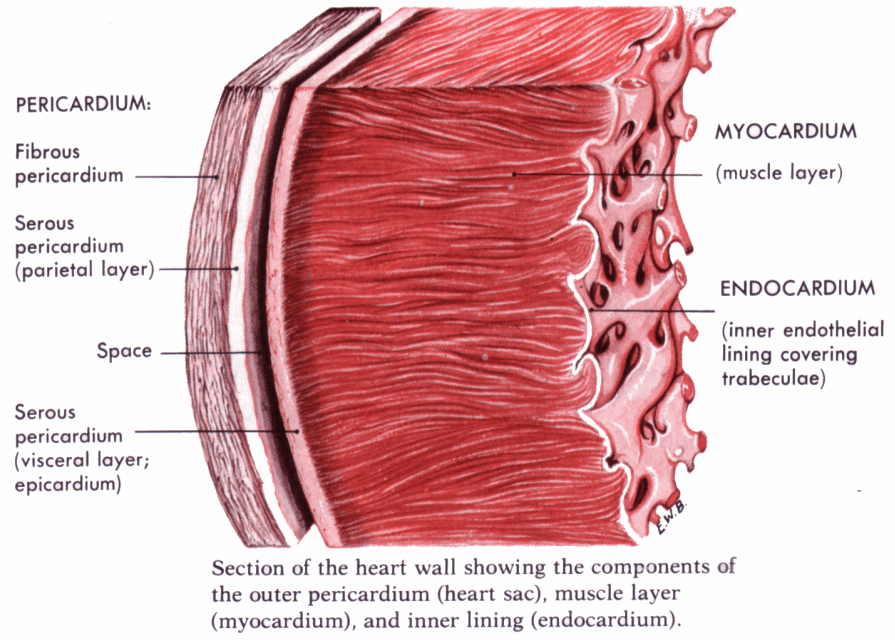

Figure 1.3: Structure of the human heart wall (taken from http://stevegallik.org/sites/histologyolm.stevegallik.org/images/heartwall.gif)

1.1.3 Excitation-Contraction coupling

The heart muscle belongs to the striated muscle with characteristics of the smooth muscle. In contrast to the skeletal muscles, the heart is controlled by the autonomic nervous system and owns center-supported cell nuclei (usually one nucleus per cell, rarely two). The heart muscle fibers come with a negative resting membrane potential. If the membrane potential increases and thereby the muscle fiber depolarizes to a certain value (threshold membrane potential) an action potential will arise. The inward flow of sodium ions and calcium ions into the muscle fibers play a very critical role for the development of the excitation. The duration of the heart action potential (a few hundred ms) is significantly longer than those of a neuron (about 1 to 2 ms). The refractory period of the heart muscle cell is long (about 300 ms). During this time no further excitation of the cell is possible. It should be mentioned that, if an excitation comes close to the end of the refractory period a number of heart muscle cells might not be excitable. This leads to a coordination loss due to premature re-excitation and is called ventricular fibrillation. Figure 1.4 shows the shape and phases of the heart action potential. Accumulations of particularly sophisticated heart muscle cells operate as excitation forming system. Changes in the resting membrane potentials occur automatically in these muscle cells (no nerves are necessary). The excitation propagation from the base to the top of the heart takes place in five steps:

1. Sinoatrial node
   acts as primary pacemaker with a frequency of 60–80 beats/minute

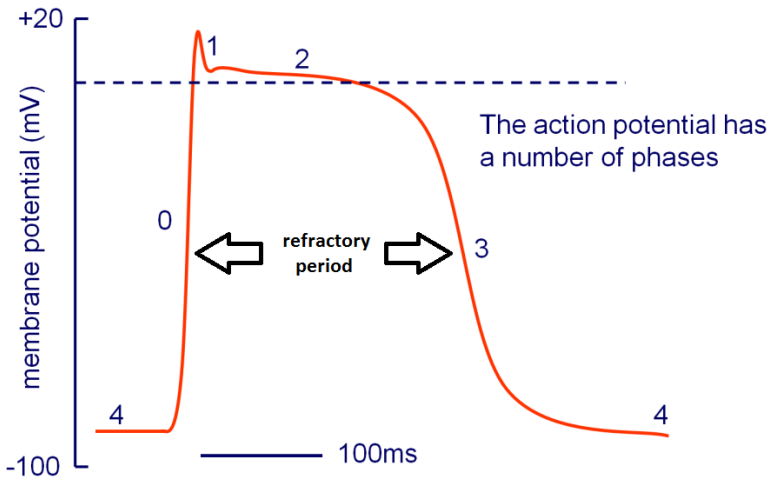

Figure 1.4: Shape and phases of the heart action potential (image adopted from http://medquarterly.com/mq88/MQIMAGES/Notes/Biochemistry)
0: rising phase, sharp rise based on the influx of sodium ions; 1: voltage decay due to sodium channel inactivation and outflow of potassium ions; 2: plateau phase, based on the opening of the calcium channels; 3: repolarization phase, voltage decay due to sodium channel inactivation and outflow of potassium ions; 4: resting membrane potential (about -90 mV)

2. Atrioventricular node
   acts as secondary pacemaker with a frequency of 40–60 beats/minute
3. His bundle
4. right and left atrioventricular bundle branches
5. Purkinje fibers
   and thus in the contractile heart muscle cells

The action potentials of the heart muscle fibers lead to an activation of the contractile elements of the heart muscle fibers. It is known as electromechanical coupling and is primarily done by the calcium-induced calcium release mechanism (Speckmann and Wittkowski (2004)).
In detail, the contraction is explained by the cross-bridge cycle between actin and myosin filament proteins. Actin is the outer and thin filament, whereas myosin is the inner and thick filament of the sarcomere. The sarcomere itself is the smallest functional unit of the myofibril and, thus, of the muscle. Figure 1.5 shows the strict organization of the sarcomere. In the resting state, the actin filament is wrapped with tropomyosin fibers which cover the binding sites of the myosin head on the actin filament. An incoming action potential ensures that the intracellular Ca^{2+} concentration rises slightly. The calcium ions enter the cell during the early plateau phase primarily by calcium channels. Due to the increase of

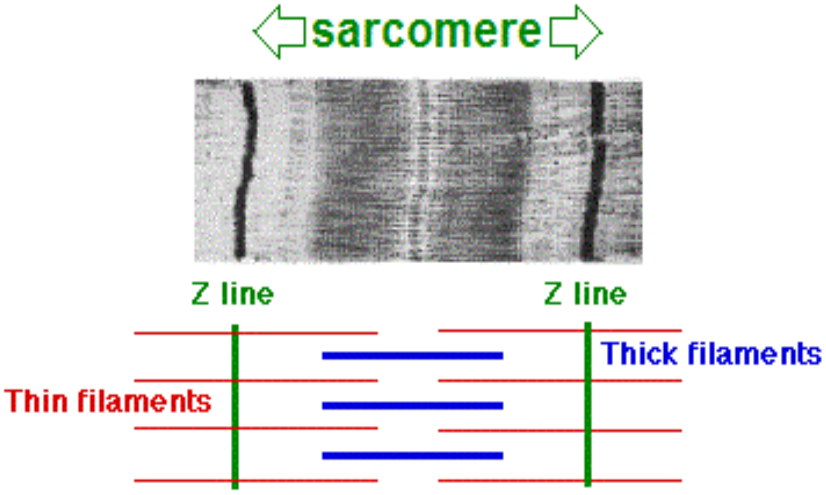

Figure 1.5: Organization of the sarcomere (taken from http://commons.wikimedia.org/wiki/File:Sarcomere.gif); upper figure: organization with the help of an electron microscope, lower figure: schematic organization

the intracellular Ca^{2+} ions, which are detected by a receptor, more calcium ions will be delivered. This positive feedback is called calcium-induced calcium release. The calcium attaches to Troponin which is linked on the tropomyosin fibers and changes the configuration of the actin binding sites, allowing myosin to bind on the actin filament. The myosin head pulls the actin filament in the center direction of the sarcomere using ATP hydrolysis. This is called contraction. Afterwards, the intracellular calcium concentration decreases by various mechanisms (mainly by sodium-calcium exchanger). This results in the myosin head dissolving from the actin filament and terminating the contraction. Now, both proteins have returned to the initial state (Hick and Hick (2006)).

2 Materials and Methods

The second chapter of this Master's thesis deals with the methods utilized. First, the specimen preparation process will be explained. Then, the experimental setup is described. At the end of this chapter some information about the general test procedure and the statistical analysis will be given.

2.1 Preparation and storage of the tissue

This chapter examines the way of the human heart from the Medical University of Graz to the dissect table in the laboratory and finally to the tensile testing machine. First, some information about the ventricular tissue and the storage of the myocardium will be given. Afterwards, the sample preparation process will be explained.

2.1.1 Ventricular tissue

We obtained the human hearts, respectively parts of them, from the Division of Transplantation Surgery, Medical University of Graz, which also provided information about age, gender, weight, and the pathological state of the donor hearts. Only hearts which were classified as non-failing were accepted. The use of human tissue was approved by the Ethics Committee of the Medical University of Graz. Nothing but myocardial strips without tissue cracks of the left ventricle (preferably the anterior wall) were used for the experiments. Figure 2.1 shows the myocardium of the left heart and its division into anterior and posterior segments using an apical two chamber view.
The following Table 2.1 gives information about the anamnesis of the donor hearts. In total four hearts were received. The fourth heart was restricted by the Ethics Committee and therefore no patient data is available. Depending on the size of the received tissue, one or two specimens were tested from each heart.

Tissue storage

Tissue damages should be kept as low as possible between the extraction of the heart and the testing in the laboratory by the use of optimal tissue storage. Due to cell dying, time plays a highly important role in working with viable human myocardium. The human organism can only stay alive for a few minutes after a cardiovascular arrest without life-saving measures. Individual organs may survive much longer in low tempered (temperature

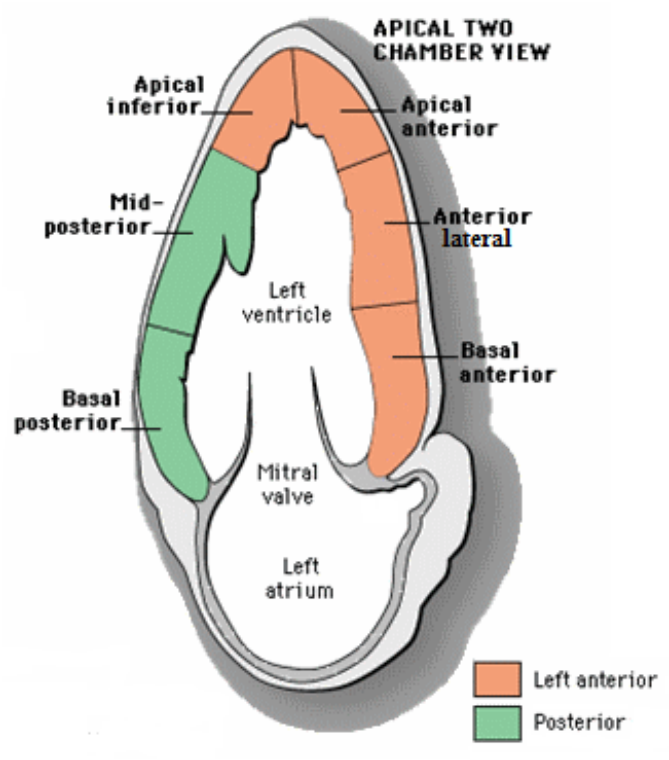

Figure 2.1: Segments of the left myocardium (image adopted from http://drsvenkatesan.com/tag/rotation-of-heart-and-q-waves)

of about 4 °C to delay biochemical processes) preservation solutions. The reversible survival time of single organs without circulation is called ischemic tolerance. The ischemic tolerance of organs can be significantly increased with the help of the following methods (heart up to 10 hours, liver up to 24 hours, kidney up to 30 hours) by

- changing the electrolyte concentration in the perfusion/storage solution,
- adding buffer systems which intercept the intracellular built acid metabolites during anoxia,
- the allowance of two-valued ions to stabilize the cell membrane,
- osmotic carrier substances to minimize the cell swelling,
- the removal of calcium ions to inhibit the excitation-contraction coupling, and
- pharmaceuticals (Reidemeister (1998)).

Therefore, the two key principles of an organ conservation solution are the minimization of the energy requirements by cell inactivation and the optimization of anaerobic energy generation by artificial buffering (Custodiol (2011)).

Table 2.1: Anamnesis of the donor human hearts (F, female; M, male; AP, apical posterior wall; LA, lateral anterior wall; PE, pericardial effusion; MD, inferior myocardial damage; CH, cerebral haemorrhage; Time, hours between extraction of the tissue and arrival in the laboratory)

	Heart number			
	1	2	3	4
Age	67	61	-	-
Sex	M	F	M	-
Sample location	AP	LA	LA	LA
Heart weight (g)	537	258	864	810
Time (h)	4.5	1.5	4	1.25
Ejection fraction (%)	65	55	-	-
Pathological state	PE	non	MD	-
Cause of death	CH	CH	-	-

Three cardioplegic solutions are well suited for the human heart preservation: the Euro-Collins solution (Collins and Wicomb, 1983), the University of Wisconsin (UW) solution (Belzer and Southard, 1988), and the Custodiol® solution (Bretschneider et al., 1975). The above mentioned fluids are characterized by high potassium and magnesium but low sodium and chloride concentrations (called intracellular solutions), compared to blood, to reduce ion shifts across the membrane. The UW solution has largely replaced the Euro-Collins solution and leads to a quick cardiac arrest. The UW is also available in an extracellular composition (low potassium and high sodium concentrations). This results in a slower cardiac arrest similar to the Celsior (Menasche et al., 1994) preservation solution. Custodiol® is a HTK (H = Histidine, T = Tryptophan and K = Ketoglutarate) fluid. Histidine acts as a buffer even at hypothermia. Tryptophan prevents the intracellular influx of histidine, and ketoglutarate is used as an energy-rich substrate. Custodiol® contains also mannitol with the ability to bind free radicals. The electrolyte composition should ensure the homoeostasis of the cell. Only Custodiol® is approved worldwide for human heart preservation (Erhard et al. (1995), Ziemer and Haverich (2011)).
The Medical University of Graz, and thus we, used Custodiol® for the storage of the heart. Compared to the UW and the Celsior solution, Custodiol® is cheap and has been used over two million times for cardiac interventions in Europe (Custodiol (2014)). In literature, it is rarely mentioned which cardioplegic solution was used. Bavendiek et al. (1998) and Brixius et al. (2001) utilized Custodiol® to perform their experiments. In many cases, Tyrode's solution supplemented with cardioplegic additives was used. Table 2.2 shows the qualitative and quantitative composition of 1000 ml Custodiol® in sterile water.
The Medical University added 21 mmol 2,3-butanedione monoxime (known as BDM) to the Custodiol® cardioplegic solution. $C_4H_7NO_2$ is the elemental formula of BDM with a molar weight of 101.1 g. Irreversible damages occur by cutting the human heart. There-

Table 2.2: Composition of 1000 ml Custodiol® (Custodiol (2011))

Component	Weight (g)	Amount of substance (mmol)
Sodium chloride	0.8766	15.0
Potassium chloride	0.6710	9.0
Potassium hydrogen 2-Ketoglutarate	0.1842	1.0
Magnesium chloride $\cdot$ 6 H_2O	0.8132	4.0
Histidine $\cdot$ HCl $\cdot$ H_2O	3.7733	18.0
Histidine	27.9289	180.0
Tryptophan	0.4085	2.0
Mannitol	5.4651	30.0
Calcium chloride $\cdot$ 2 H_2O	0.0022	0.015

fore, BDM is used to protect the tissue from too severe damage. Tissue which has been treated with BDM for about 30 minutes before cutting shows significantly higher twitch stresses/forces than untreated human myocardial specimens. It is assumed that BDM reduces the cutting injuries by a decrement of contraction which comes from cutting the cell membrane and a reduction in the sensitivity of the contractile proteins to calcium ions. BDM seems to be able to protect the myocardium against oxygen deficiency and is an effective, rapid acting, and reversible inhibitor of cardiac contractility. The amount of BDM substance used ranges, in most cases, from 30 to 50 mmol, although 20 to 25 mmol seem to be sufficient for the protective effects. For this reason and because of the time factor, no further BDM was added to the solution (Mulieri et al. (1989)).

2.1.2 Preparation

The human heart was collected at the Center of Medical Research, Medical University of Graz. The tissue was then transported to the laboratory in cooled Custodiol® cardioplegic solution with BDM to ensure optimal chances of survival. The time factor has always played an important role in the execution of the experiments. According to various papers, cardiac tissue is able to survive up to 10 hours in cardioplegic solution (Mulieri et al. (1992), Holubarsch et al. (1998), Camelliti et al. (2011)). This period of time could always be adhered to (see Table 2.1).
First of all, the connective tissue and the fat were removed from the left ventricle. After that, a thin slice (about 1.5 to 2 mm thick) was cut off with the help of an electrical universal cutter. It was demanding to get suitable and uniform slices because of two reasons: first, the bulky cutter made it hard to get thin slices and second, the very soft myocardium was difficult to handle. Yet, thin slices are essential because of the diffusion-based nutrients supply of the heart muscle fibers. Basically, it was planned to cut the tissue parallel to their muscle fiber direction. This was however, rarely possible because the fiber direction was hard to see and the obtained myocardial tissue piece was in most cases rather small and

had to be cut in the predetermined directions. Because of this reason, the tested specimens were engaged in formaldehyde after the experimental task to be able to determine the fiber direction.
A rectangular specimen with a width of about 8 mm and a test length of about 20 mm was cut out of the thin slice. Small pieces of sandpaper were glued to both ends of the individual sample with instant adhesive. Super-glue flowing onto the sample testing region had to be avoided as it could have altered the mechanical behavior and reduced the survival time. The main function of the sandpaper was to ensure that the specimen did not slip out of the clamps of the tensile testing machine. It was also easier to clamp the sample to the desired position. A schematic view of the specimen can bee seen in Fig. 2.2.

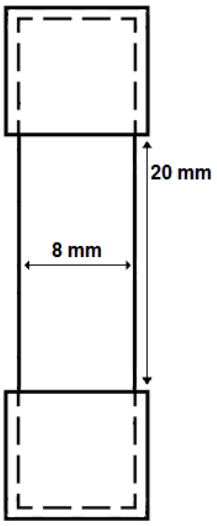

Figure 2.2: Schematic view of the specimen with pieces of sandpaper on both ends

The sample preparation was completed by applying a random particle pattern on the specimen by spraying a special tissue marker with an airbrush set. The resulting pattern was required to measure the two-dimensional strain of the specimen by a video extensometer. To receive suitable pictures, a pellucid solution was essential. Therefore, the measurement was only performed when the pellucid Tyrode nutrient solution was available. Table 2.3 shows the dimensions of the tested specimens and gives information on what kind of solution was used. A prepared sample can be seen in Fig. 2.3. After spraying the specimen, it was placed in the testing solution to ensure an optimal nutrient and oxygen supply.

2.2 Experimental setup

In the following section the experimental setup is explained. The focus is set on the hardware, essential to the measurement of the mechanical properties of biological tissue, in-

Table 2.3: Dimensions of the tested specimens (NM, not measured)

	Specimen 1		Specimen 2		Solution
	Width (mm)	Thickness (mm)	Width (mm)	Thickness (mm)	
Heart 1	NM	NM	-	-	DMEM
Heart 2	7.50	1.50	8.00	2.20	DMEM
Heart 3	NM	NM	NM	NM	Tyrode
Heart 4	8.50	1.80	8.30	1.80	Tyrode

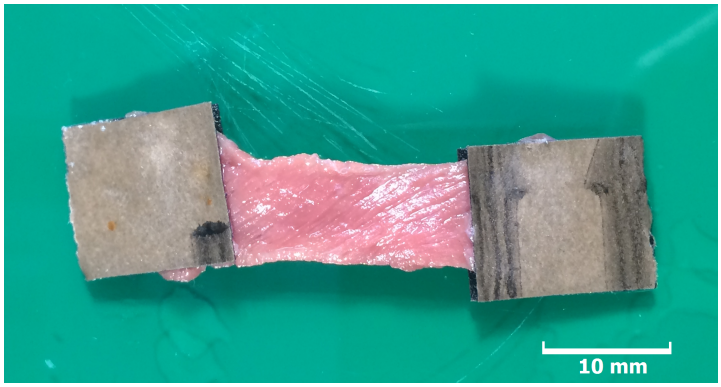

Figure 2.3: Prepared specimen with sandpaper glued on the edges and before spraying

cluding their control software. Information about the tensile testing machine, the nutrient solution and further used components will be given.

2.2.1 Uniaxial tensile testing machine

To measure the mechanical properties (force respectively stress) of human tissue in uniaxial direction, an uniaxial tensile testing machine for small biological specimens was required. In the specific case, the tensile testing machine was used to measure the twitch force of the sample when an electrical stimulus was applied. The supervision of the machine is computer controlled. Figure 2.4 shows the schematic construction of the tensile testing machine.
As can be seen in Fig. 2.4 the main components are:

- load cell
- upper and lower crosshead
- external digital controller
- acrylic glass container
- fixing clamps

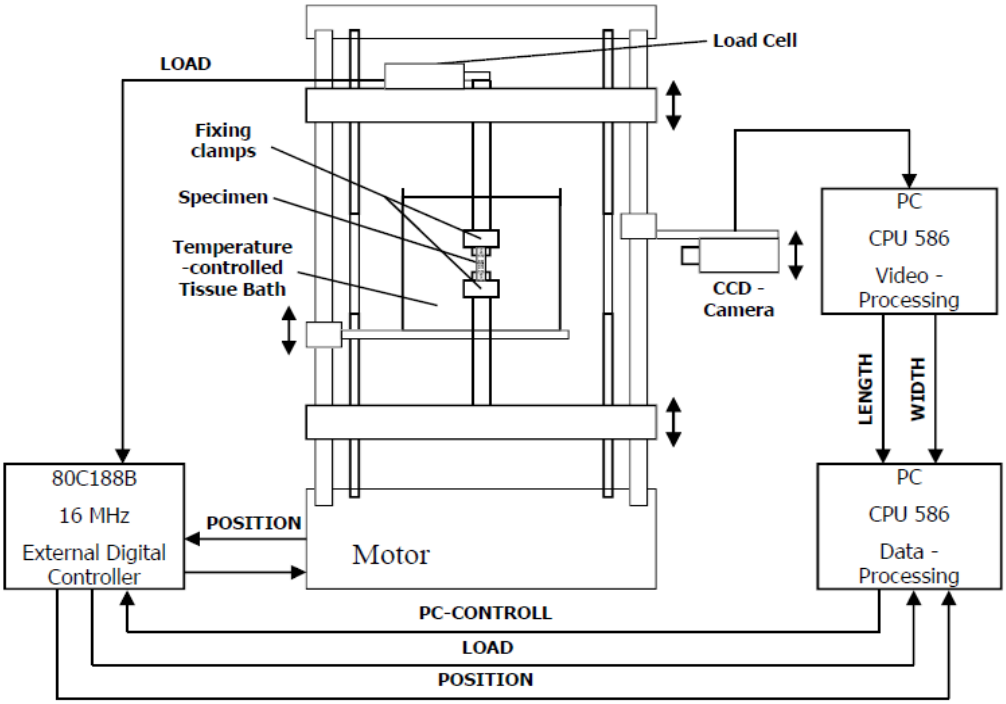

Figure 2.4: Schematic construction of the tensile testing machine (Sommer et al. (2008))

- video extensometer
- PC for data processing

The load cell was required to measure tensile, respectively twitch force. For the experiments, a 10 N class 1 strain-gauge load cell (model F1, AEP transducers) with a load resolution of 1 mN was used. The upper and lower crosshead of the tensile testing machine moved in opposite directions to ensure that the sample remains in the same range of vision (stroke resolution of 0.04 μm). The task of the external digital controller (model EDC 25/90W, DOLI; Munich, Germany) was to regulate the electric drive of the machine. The data collection of the load and crosshead position was controlled by the digital controller. Since it is important to simulate physiological conditions when testing mechanical properties of biological tissue, an acrylic glass container, filled with nutrient solution was used to ensure the specimen was supplied with necessary substances. While conducting the experiments, the specimen was fixed between the two clamps and was surrounded by the acrylic glass container. A circular water heater (model: E 200, Lauda; Lauda-Königshofen, Germany) was used to maintain a temperature of 37°C of the nutrient solution by placing the heating coil into the tissue bath. The plexiglass container and the heating coil were manufactured by the Institute of Hydraulic Engineering and Water Resources Management, Graz University of Technology. The computer collected the data of the measurement process and allowed a real-time recording of the measured values. Figure 2.5 shows the measurement

arrangement in the laboratory.

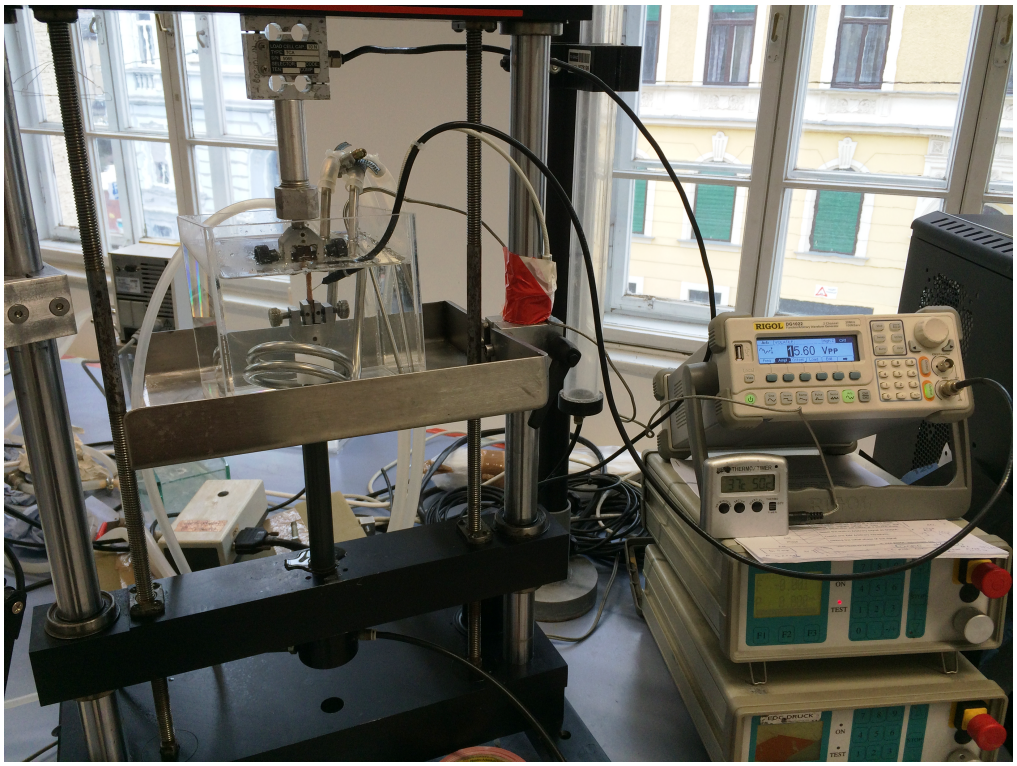

Figure 2.5: Measurement arrangement in the laboratory; left: acrylic glass container filled with nutrient solution and specimen in contact with the Pt-micro-electrode fixed between the clamps of the uniaxial tensile testing machine; right: external digital controller and function generator

2.2.2 Nutrient solution

While performing the experimental task, a nutrient solution is necessary to reach a duration of survival of a few hours by supplying the tissue with the required substances. Two different solutions were used: the Tyrode's solution (also known as Krebs-Ringer solution) and the Dulbecco's modified Eagle's medium (DMEM). The latter was only used when no Tyrode's solution was available.
The Tyrode's solution is a fluid of electrolytes in physiological composition. It contains sugar as an energy source and bicarbonate as a buffer. It is used for cell culture applications and physiology experiments with living tissue (usually gassed with 95% Oxygen and 5% Carbon Dioxide). It is named after its inventor Maurice Vejux Tyrode, an American pharmacologist (Pschyrembel (2004)). The Tyrode's solution was blended at the graft surgery laboratories of the Medical University of Graz.
1000 ml of the stock solution contains the following components:

- 138.4 g $NaCl$
- 7.0 g KCl
- 3.2 g KH_2PO_4
- 2.8 g $MgSO_4$ or 5.8 g $MgSO_4\ 7H_2O$
- 7.4 g $CaCl_2\ 2H_2O$

The stock solution is mixed as follows: first, prepare an Erlenmeyer flask and a magnetic stir bar. Then pour 700 ml MilliQ H_2O (an especially purified water) into the flask and add the salts in the above given order. It is very important that the last added salt is completely dissolved before the next component is added to the solution. Meanwhile, $CaCl_2\ 2H_2O$ and 50 ml MilliQ are stirred in a separate flask until the mixture is transparent. The $CaCl_2\ 2H_2O$ mixture and 250 ml MilliQ water are added to the 700 ml alloy by agitating the flask to finish the stock solution. Finally, the stock solution has to be filtered. It can be stored in the refrigerator in a brown glass bottle (to protect the solution from light) for up to two weeks.
To get 2000 ml Tyrode's solution following components are required:

- 100 ml stock solution
- 1900 ml MilliQ H_2O
- 4.4 g $NaHCO_3$
- 4.2 g dextrose (D-glucose)

The blending of the Tyrode's solution is similar to the stock solution: first, $NaHCO_3$ is completely dissolved in 500 ml MilliQ water. Afterwards, the dextrose is added under swinging. Then 100 ml of the refrigerated stock solution are added to the alloy diluted with 1400 ml MilliQ H_2O to get the Tyrode. Finally, the pellucid solution has to be filtered. A major disadvantage of the Tyrode's solution is that it has to be used within 24 hours after manufacture. In nearly every paper dealing with experiments on human ventricular myocardium the Tyrode's solution is used to ensure the viability of the tested tissue (Mulieri et al. (1992), Schwinger et al. (1993), Holubarsch et al. (1998), Brixius et al. (2001), Camelliti et al. (2011), Brandenburger et al. (2012), etc.).
When the Tyrode's solution was not available the proprietary prepared DMEM solution was used. DMEM is a standardized culture medium which is utilised in human and animal cell culture applications. According to the specifications by the manufacturer, the DMEM should solely be used for cell culture applications and not for physiology experiments (no papers could be found in which DMEM was used for human ventricular myocardium experiments) with living tissue. The DMEM is a modification of the Eagle's minimal essential medium (EMEM). EMEM contains the following components:

- amino acids
- salts (almost the same salts as in the Tyrode but in different concentrations)

- glucose
- vitamins

DMEM contains approximately four times as much of the amino acids and vitamins, a two- to four-fold higher concentration of glucose, and some additional supplementary components compared to EMEM. While the Tyrode's solution is transparent, DMEM is a reddish solution (Pombinho et al. (2004)) which was used only for the experiments on the first two hearts.

2.2.3 Further components

The following further components were required to accomplish the experimental setup:

- video extensometer
- function generator
- Pt-micro-electrode
- carbogen gas supply
- airbrush pistol

The computer-based video extensometer (model ME 46-350, Messphysik) was used to optically measure the thickness of the specimens by utilizing a charge-coupled device camera. It was additionally used for recording an image series to gather information about the two-dimensional strain. The device sent the measured values in real time to the video processing unit and subsequently to the PC. The black and white contrast of the specimen's surface and the background was a necessity for the measurement.
An arbitrary function generator (model Rigol DG1022) was required for the generation of the electrical stimulus. To receive the desired output signal the waveform generator had to be programmed. The Rigol DG1022 generator is characterized by its large frequency range (1 μHz – 20 MHz) and its short ramp-up time ($<$ 20 ns). Therefore, it is optimally suitable for the experimental task. The generator was borrowed from the Institute for Electronics, Graz University of Technology.
A purpose-built (manufactured by the Institute for Electronics, Graz University of Technology) platinum-micro-electrode was used to deliver the electrical stimulus to the tissue. The Pt-wires of the micro-electrode had a diameter of 250 μm. The gap between the reference pole and the active pole (known as bipolar electrode) was roughly 1.5 mm. Platinum micro-electrodes were used in most of the contractile tissue experiments (Sonnenblick et al. (1965), Mulieri et al. (1992), Schwinger et al. (1993), Brixius et al. (2001), Brandenburger et al. (2012), etc.) mainly because platinum remains inert during the electrolysis. The utilized electrode can be seen in Fig. 2.6.
To supply the tissue with oxygen a 95% O_2 and 5% CO_2 gas mixture was used. This mixture is referred to as Carbogen and is well used in cell culture and tissue experiments. Unfortunately, it was only possible to ensure the gas supply in testing breaks because the

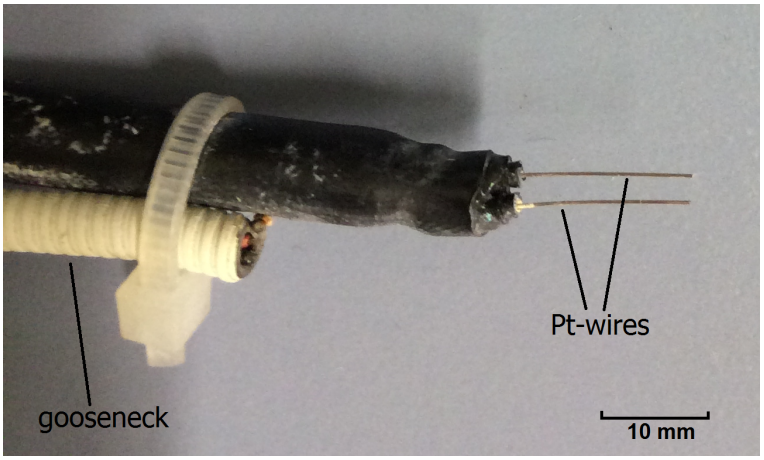

Figure 2.6: Pt-micro-electrode with the two Pt-wires and gooseneck for flexible positioning of the electrode

gas bubbles exerted a force on the load cell.
The airbrush pistole (model Double Action Airbrush HP-101) was used to spray the specimen with black color. The result was a kind of speckle pattern which might be required to measure the two-dimensional strain of the tested specimen with the help of the video extensometer.

2.3 Test procedure

The general test procedure will be explained in detail in this chapter. Then some information about the data preparation process will be given.

2.3.1 General procedure

At the very beginning, the human ventricular myocardium was prepared as described in section 2.1. At least one specimen per heart, or two if the ventricular tissue piece was large enough, was tested. The remaining myocardium was currently stored in an frigid cardioplegic solution with BDM to ensure best survival conditions. Before conducting the experiments, the tensile testing machine and the further components had to be arranged. The acrylic glass container was filled with nutrient solution and heated up to 37 °C by a circular water heater. The function generator was prepared for use and connected to the platinum electrode. At last, the nutrient solution, respectively the specimen, was supplied with a 95% O_2 and 5% CO_2 gas mixture.
After all components were ready to use and the sample preparation process was finished, the specimen was clamped into the tensile testing machine. The clamping process led to more or less serious problems: clamping too tight induced tissue injury, whereas clamping

too loose caused the specimen to slip from the clamp. Therefore this procedure had to be performed rigorously.

Threshold voltage and steady state

Initially, it was important to determine the threshold voltage and reach the steady state. The specimen was clamped in a way no force acted on the tissue which was surrounded by nutrient solution. The following steps were made to ensure a force-free state: the specimen was only fixed at the upper clamp. The acrylic glass container, filled with nutrient solution, was moved up to immerse the sample with fluid. The force was set to 0 N, because this corresponded to the force-free state when the tissue was surrounded by solution. The specimen was fixed at the lower clamp and again immersed with nutrient solution. The clamps were then moved towards or apart from each other until the displayed force coincided to 0 N, corresponding to the force-free state.
The specimen was brought in contact (approximately in the middle of the sample) with the Pt-micro-electrode to deliver the electrical signals. To ensure a flexible positioning of the electrode a gooseneck was used. The stimulation voltage was increased in steps of 0.5 V starting from 0 V up to the point the specimen showed a contraction and a twitch force could be measured by the load cell. This voltage is called peak to peak 'threshold voltage'. The 'stimulation voltage' is defined as the by 20% increased 'threshold voltage' and can be calculated as:

$$\text{stimulation voltage} = \text{threshold voltage} \cdot 1.2\ . \tag{2.1}$$

This 'stimulation voltage' (peak to peak) was used for all further experiments of the individual specimen. To determine the 'threshold voltage' the frequency was set to 0.1 Hz and the pulse width to 5 ms on the function generator. Basically, a biphasic stimulation impulse was used in all experimental tasks as shown in Fig. 2.7. This direct current (DC) impulse is characterized by its consecutively applied positive and negative rectangular shaped pulse of the same length. Therefore a shift of the ions across the cell membrane should be avoided to protect the tissue against damage. The biphasic stimulation impulse is well used in human myocardial slice experiments.
Once the steady state had been reached, there was no further increase in the specimen's twitch force (washing out the cardioplegic solution with BDM from the myocardium). The following biphasic impulse parameters had been used until the steady state was reached: 0.1 Hz frequency, 5 ms pulse width and the aforementioned stimulation voltage. It should be mentioned that the electrode position on the individual specimen was not changed during the whole experimental task (including stress/force-frequency relationship and control measurements).

Stress/force-frequency relationship

To gather information about the stress/force-frequency relationship, the pulse width (5 ms) and the stimulation voltage were held constant during this experimental task. The stimula-

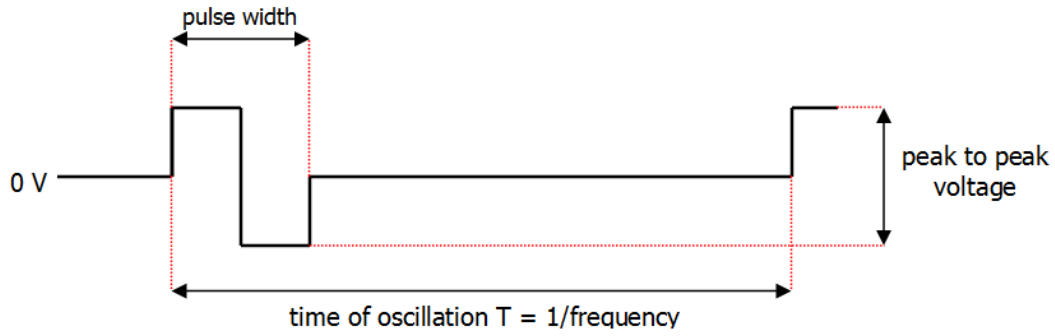

Figure 2.7: Biphasic stimulation impulse with the definition of the adjusted stimulation parameters (pulse width, time of oscillation, and stimulation voltage) on the function generator

tion frequency was usually increased in five minute intervals (except for specimen two of the fourth heart, where the intervals were 100 s) as follows: 0.1 Hz, 0.3 Hz, 0.5 Hz, 1 Hz, 1.5 Hz and 2 Hz. After all frequencies have been applied, the specimen was pre-stretched to 50 mN and 100 mN. In the pre-stretched condition the frequency was again increased in five minute intervals. Due to the excessive noise level the Carbogen supply was maintained only during experimental breaks. The measurement software enabled to view the real time data, as can be seen in Fig. 2.8.

Strain measurement

An image sequence (duration of approximately 10 s) was taken by the video extensometer during each of the stimulation frequency intervals and pre-stretches (0, 50 and 100 mN) to gather information about the two-dimensional strain. It was only recorded when the pellucid Tyrode's solution was available. The time between two pictures was 25 ms. This resulted in a resolution of 40 images per second. In order to achieve better contrast the specimen's surface had been sprinkled with black color. Figure 2.9 shows a single picture of an image series. It was absolutely necessary to rotate the acrylic glass container in a way it was normal to the video extensometer to avoid errors caused by geometrical distortion.

Control experiments

The influence of the pulse width on the twitch force had to be investigated. For this reason the stimulation voltage and the frequency (set to 0.5 Hz) were held constant. The specimen was stimulated primarily 5 minutes with the 'normal' pulse width of 5 ms and then 5 minutes with a width of 2.5 ms without pre-stretch of the sample.
In addition, the influence of the stimulation voltage on the twitch force should be explored. Therefore the pulse width (set to 5 ms) and the frequency (set to 0.5 Hz) were kept constant. The sample was stimulated firstly 5 minutes with the 'normal' stimulation voltage and after

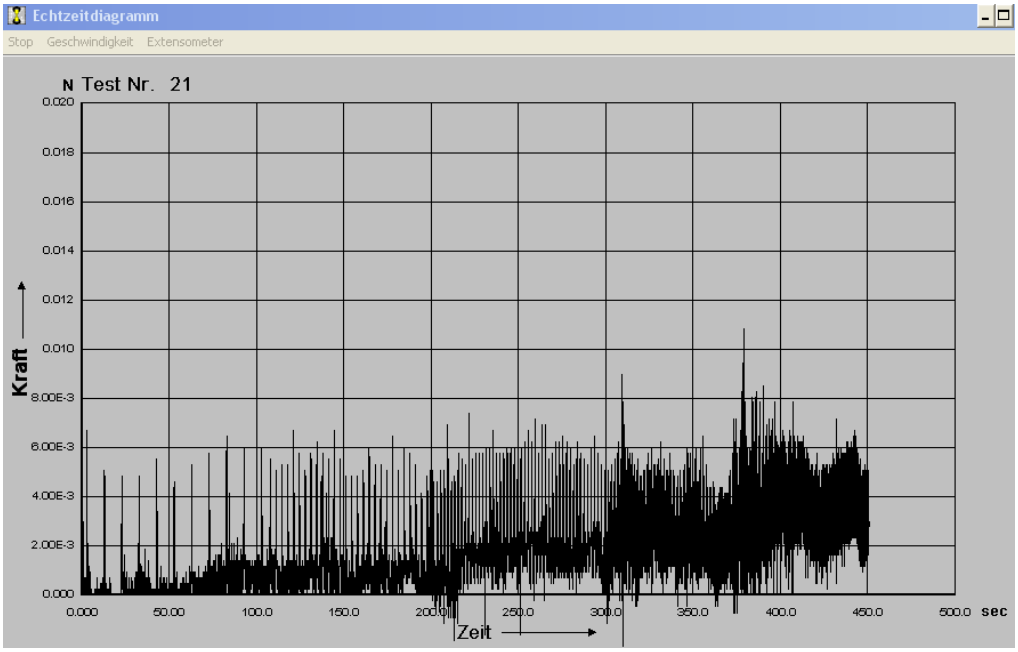

Figure 2.8: Real-time view of the force-time diagram; twitches correspond to the reaction of the myocardium (activation of the muscle fibers) as a consequence of an electrical stimulus

this 5 minutes with a 50% increased stimulation voltage without pre-stretch of the sample. Purely out of interest, the electrode was placed in the nutrient solution without contact to the specimen to see whether or not the tissue would contract.

Thickness/width measurement

After finishing the experiments the thickness and width of the specimen was measured. The sample was laid on a black colored objective carrier and was gauged with the help of a video extensometer. Calibration had to be done to ensure the two parameters were measured correctly. To keep the stochastic error as little as possible, the thickness and width of the specimen were gauged four times, twice on each side on two different positions. Afterwards, the arithmetic mean was calculated. It was sometimes difficult to perform a correct measurement because a number of samples showed a tendency to coil. In the next step, a picture of the specimen was taken by a Canon DSLR camera.

Histology

The tested specimens were stored in 4% buffered formaldehyde solution (pH 7.4) for histological investigations at the Institute of Pathology, Medical University of Graz. Histological studies were performed on formalin fixed and paraffin embedded cuts in the plane

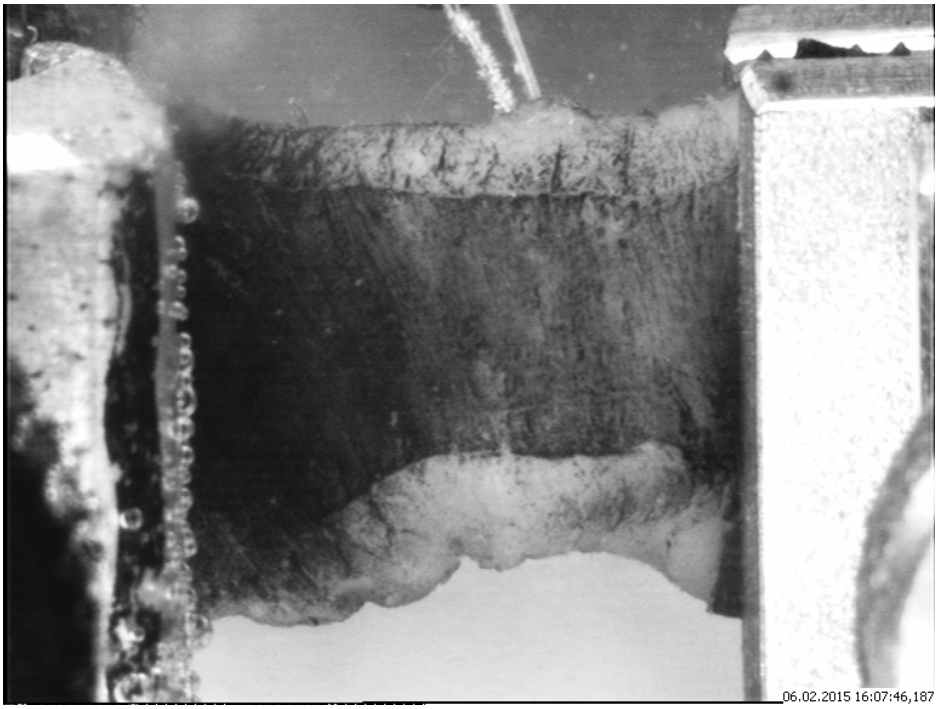

Figure 2.9: Recorded picture from an image series; the sprinkled specimen is fixed between the two clamps of the tensile testing machine and in contact with the Pt-micro-electrode

of the samples. The slices were stained with Hematoxylin and Eosin (H&E) to highlight cell nuclei. A Zeiss Axio Scope A1 microscope (Carl Zeiss, Jena, Germany), set to a magnification of either 2.5× to 20×, was used to acquire images.

2.3.2 Data preparation

The measurements from the uniaxial tensile testing machine and the video extensometer had to be prepared before they could be used.

Stress/force-frequency relationship data

The tensile testing machine stored the measured values in a .dat file with the following structure: it started with the header. The measured data (time and force) was recorded after the header in a two columns structure. The header was irrelevant to further analysis and was deleted. A Matlab-Code (The MathWorks, Matlab Version: 7.7.0.471 (R2008b), 2008) was written to plot a stress/force-time diagram of the recorded values.
Equation 2.2, where F is the force, W the initial width, and T the initial thickness of the

specimen, is needed to calculate the first Piola-Kirchhoff stress P:

$$P = \frac{F}{W \cdot T} \,. \tag{2.2}$$

To gather information about the twitch stresses/forces at various pre-stretches and different frequencies a Matlab-Code (Copyright by N. C. Yoder, 2011) was adapted. The code detected the twitch peaks including consideration of the noisy baseline-shift to calculate the correct twitch stress/force. The peaks were averaged in a range of usually 200 s but at least over 5 twitches (only in rare cases, predominantly in the low frequency domain) per frequency and pre-stretch depending on the quality of the recorded values. Figure 2.10 shows a section of the peak detection. The baseline noise was relatively pronounced as can

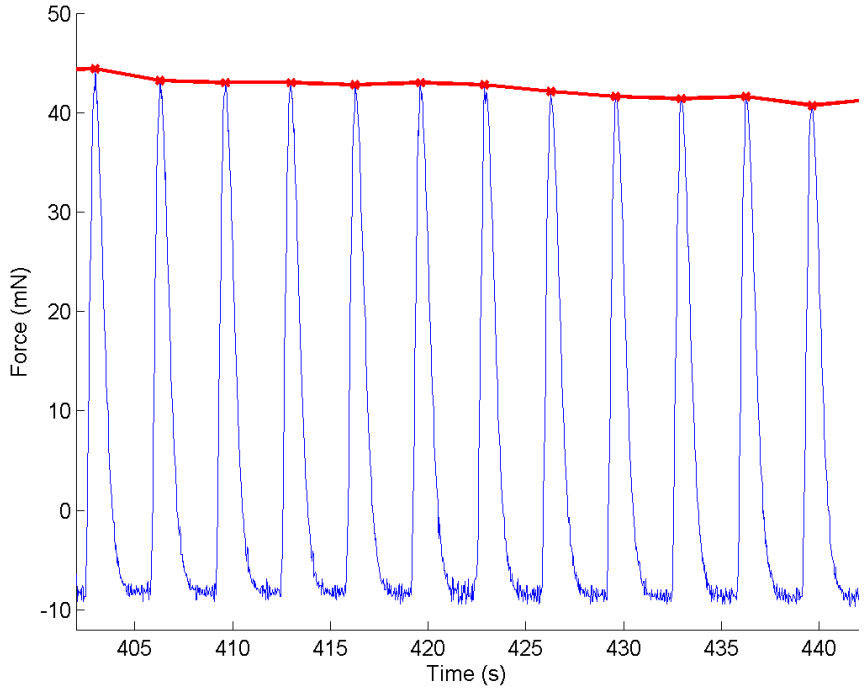

Figure 2.10: Section of the peak detection with pronounced baseline noise; twitch peaks are shown by red dots (connected by a red curve) in the force-time diagram

be seen in Fig. 2.10. The signal was low-pass filtered to quantify the baseline-shift which was then subtracted form the detected peak to receive the true twitch stress/force value. The low-pass filtered signal can be seen in Fig. 2.11.

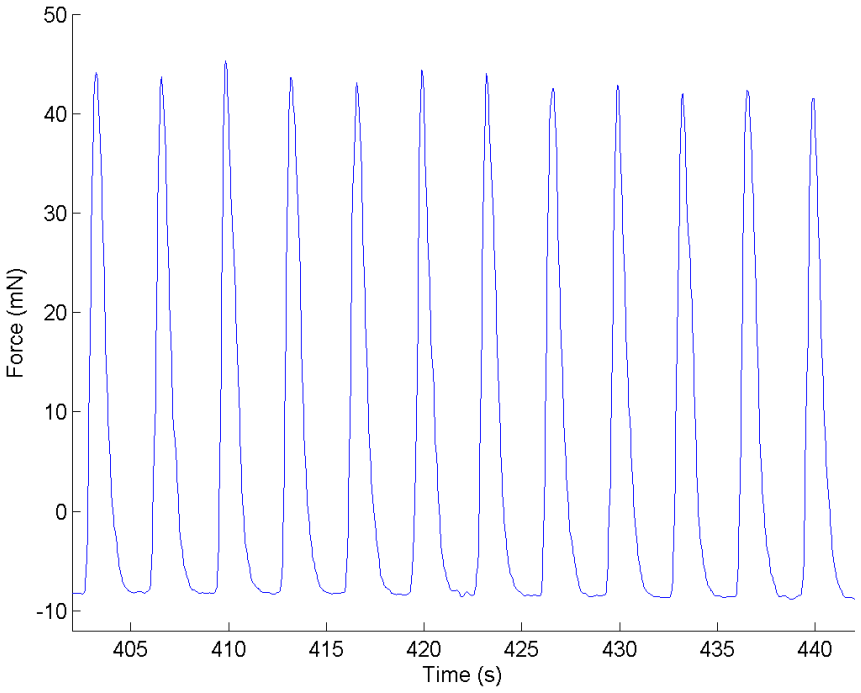

Figure 2.11: Force-time diagram of the low-pass filtered signal to quantify the baseline-shift in order to calculate the correct twitch stress/force

Twitch-time and time-to-peak data

The twitch-time and the time-to-peak were evaluated to analyze the time behavior of an electrically induced twitch. Figure 2.12 shows a single twitch and the definition of the above mentioned timing parameters. Three individual twitches were used for each pre-stretch and frequency (e.g. 50 mN and 0.3 Hz) arrangement to calculate the twitch-time and the time-to-peak by averaging.

Strain data

To evaluate the two-dimensional strain in an image sequence a Matlab-Code (Copyright by C. Eberl, D.S. Gianola and S. Bundschuh, 2010) was used. The Matlab-Code is based on the Digital Image Correlation and allows to calculate strains from a sequence of consecutive images. Following steps were necessary to estimate the strain data: first, an image series had to be selected. Irfanview (Ifran Skiljan, Irfanview Version: 4.38) was used to change the image format to the preferred .tif and also for renaming the individual pictures to achieve an ascending numbering. Depending on the twitch-time, the quantity of images was selected variably in the frequency range of 0.1 Hz to 0.5 Hz. At higher frequencies

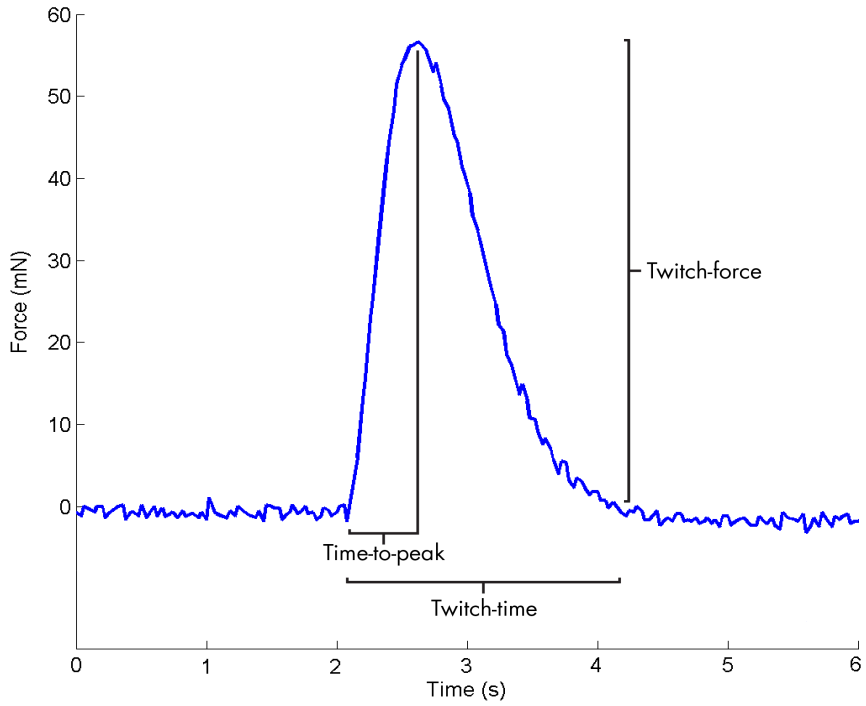

Figure 2.12: Single twitch and definition of the timing parameters

(1 Hz, 1.5 Hz and 2 Hz) the maximum time period between two twitches was chosen (1 s, 0.67 s and 0.5 s) for the length of the image series. It should be mentioned that the first picture of an image sequence represents the resting state before the stimulation impulse occurs. A grid had to be generated for the correlation process. A rectangular eleven by six grid, with the dimensions of 250 pixels in x- and 125 pixels in y-direction, was used. The grid was located in the center of the specimen as can be seen in Fig. 2.13. The definition of the coordinate system, which was necessary for the evaluation of the strain data, is shown in Fig. 2.13.
The next step was to calculate the pixel displacement in the images. Finally, the automation function did all the laborious correlation work by processing all markers and images. Then the collected displacement respectively strain data could be analyzed. To review the displacement field, delete badly tracked markers, or calculate the one- and two-dimensional strain, an included function was used.
The strain is defined as the ratio of the total deformation (pixel displacement) to the initial dimension of the specimen (grid pixel dimension). With the following Eq. 2.3 where ε is the engineering strain, L is the original length and l is the final length, the strain can be calculated:

$$\varepsilon = \frac{\Delta L}{L} = \frac{l - L}{L} = \frac{\text{pixel displacement}}{\text{grid pixel dimension}} \,. \tag{2.3}$$

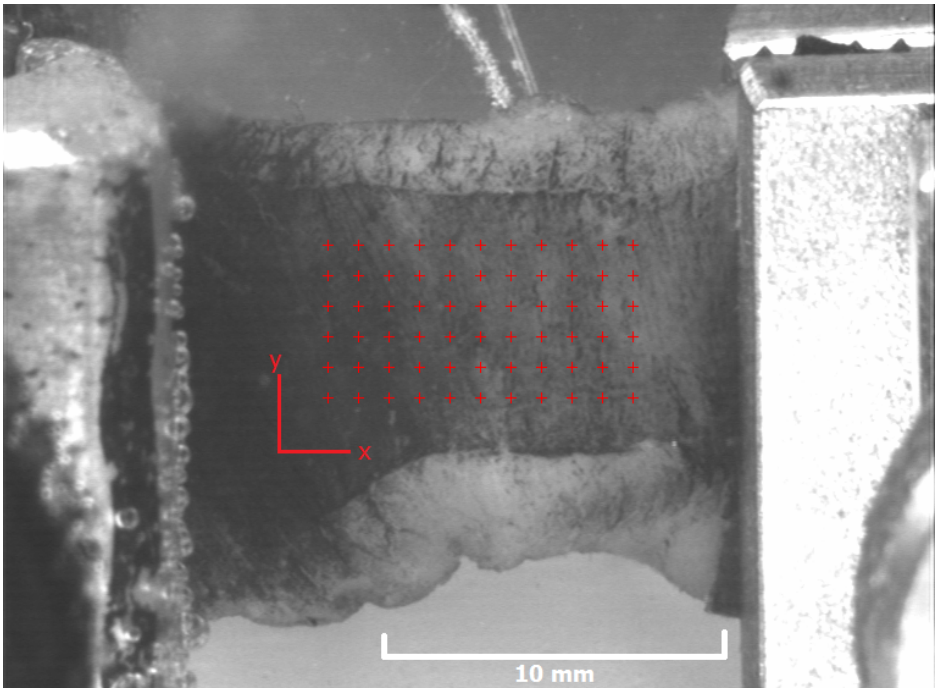

Figure 2.13: Specimen with the chosen grid used for strain calculation

The average strain is used to evaluate the one-dimensional strain of an image sequence. It was calculated by setting a regression line in the grid position-displacement plot for each picture of a series as can be seen in Fig. 2.14. The circles represent the displacement of the individual markers in reference to their initial grid positions. Therefore, the slope of the regression line corresponds to the average strain.
By the help of an image series, the time from the beginning of a contraction to the maximum average strain (called strain time-to-peak) was determined as follows. The beginning of the contraction could be clearly identified by a brightening of the Pt-micro-electrode wires in the low frequency range of 0.1 Hz to 0.5 Hz as can be seen in Fig. 2.15. The image number in which the maximum average strain occurred was detected by the included Matlab analysis function in combination with a self written Matlab Code. The strain time-to-peak was finally calculated by subtracting the recording times of the two images.

2.4 Statistical analysis

Statistical methods will be used in this Master's thesis to get a quick information about whether a distribution of a feature is remarkable or unusual. In particular, the arithmetic mean and the standard deviation will be used. The arithmetic mean is defined as the ratio of the sum of the measured values and the quantity of the values. Equation 2.4 shows the

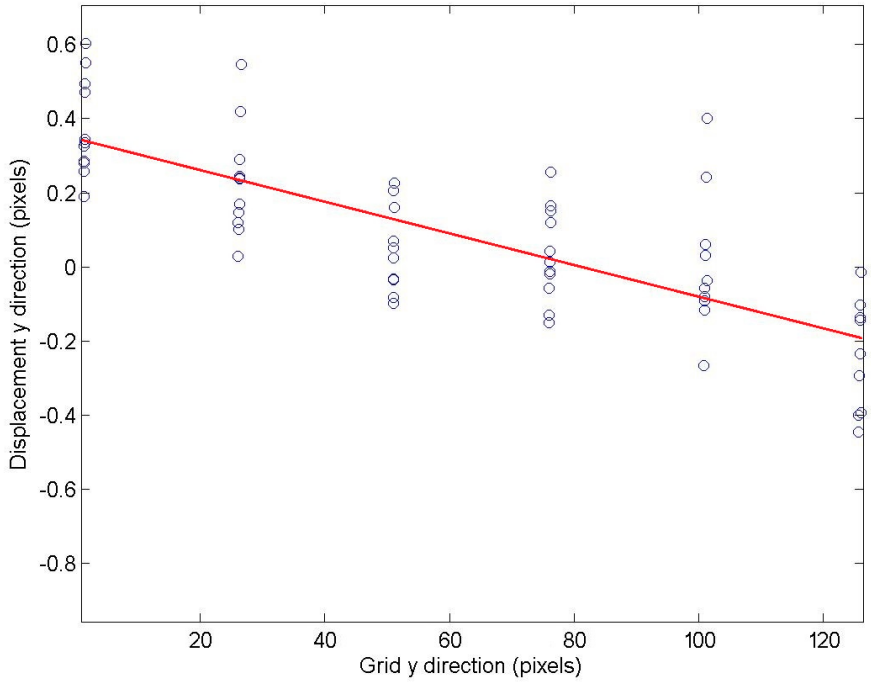

Figure 2.14: Calculation of the average strain by setting a regression line (red line) in the grid position-displacement plot

calculation formula for the arithmetic mean $\overline{x}$, where n is the number of samples and x_i is the individual sample value:

$$\overline{x} = \frac{1}{n} \sum_{i=1}^{n} x_i \ . \tag{2.4}$$

The standard deviation SD is a measure of the spread of values about its arithmetic mean. The standard deviation is defined by Eq. 2.5:

$$SD = \sqrt{\frac{1}{n-1} \sum_{i=1}^{n} (x_i - \overline{x})^2} \ . \tag{2.5}$$

To calculate the arithmetic mean and the standard deviation the statistical software R (The R foundation for statistical computing, R Version: 2.12.0, 2010) and Matlab (The MathWorks, Matlab Version: 7.7.0.471 (R2008b), 2008) were used. A normal distribution of the measured values was assumed. This was required in order to use the arithmetic mean and the standard deviation.

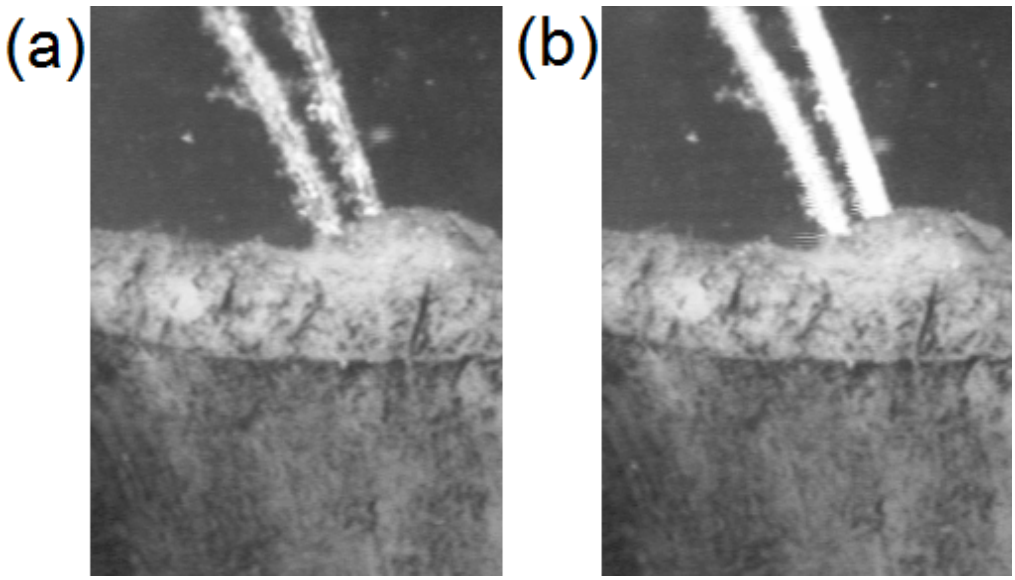

Figure 2.15: Pt-micro-electrode wires: (a) wires before contraction; (b) brightening of the wires when the stimulation impulse occurred

3 Results

In this section of the Master's thesis the experimentally measured results and prepared data will be listed. The main focus is placed on the stress/force-frequency relationship and the two-dimensional strain data of the human left ventricular myocardium. In addition, information about the threshold voltage and steady state, the twitch timing parameters, the conducted control experiments, and the histological report will be given.
In total four hearts were tested. The first heart was received, even though the experimental setup and measurement report were not finished. For this reason, the measured values of the the first heart were not objective and therefore excluded as part of the results. Nevertheless, important findings could be gained. The third heart showed no contraction thus no twitch force could be measured. The following results are based almost exclusively on the data of the donor hearts two and four.

3.1 Threshold voltage and steady state

Table 3.1 shows the threshold voltage, the time until the first contraction occurred, the time until the steady state was reached, and the storage period in the cardioplegic solution before using the tested specimens. The peak-to-peak threshold voltage varies strongly (at least by a factor of two) between the two various hearts. Compared to the others, the first specimen of the second heart took remarkably less time to contract for the first time and to reach the steady state. Additionally, the first tested samples showed a lower threshold voltage, a shorter period of time until the first contraction occurred and the steady state was reached, in contrast to the later tested specimens. Figure 3.1 shows a force-time diagram of

Table 3.1: Threshold voltage, time to first contraction, time to reach the steady state and storage time in cardioplegia of the tested specimens

	Specimen 1			
	Threshold (V)	First contraction (s)	Steady state (s)	Storage time (h)
Heart 2	4	150	500	2
Heart 4	12	1500	2000	1.75
		Specimen 2		
Heart 2	6.50	1800	2500	7.50
Heart 4	13	2000	2600	5.75

specimen two of the second heart. As can be seen in the plot, the first pronounced twitch force occurred after a stimulation period of about 1800 s. The two distinctive steps in Fig. 3.1 are due to a movement of the Pt-micro-electrode.

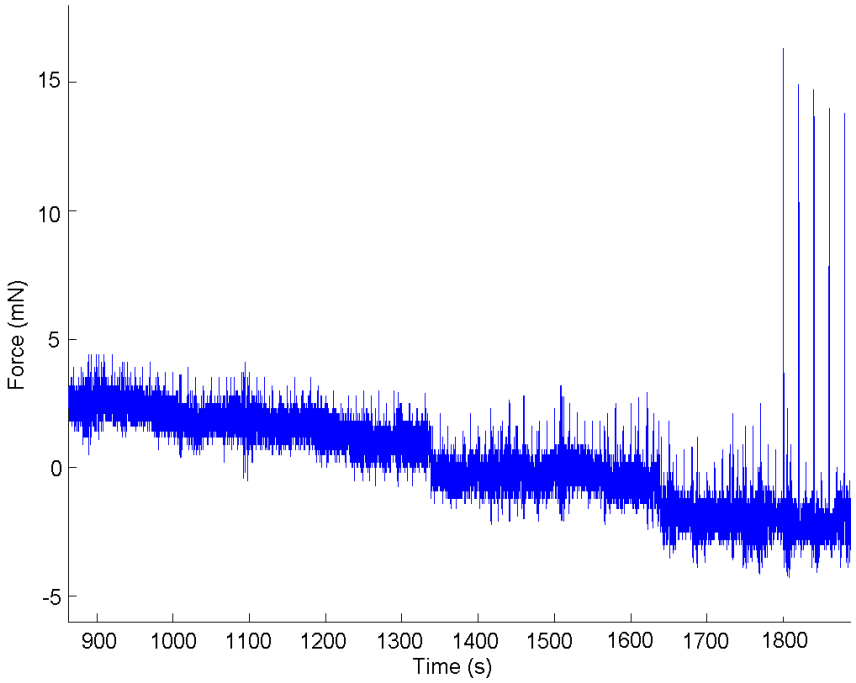

Figure 3.1: Time period until the first contraction occurred (heart 2, specimen 2); the two distinctive steps are due to a movement of the electrode

3.2 Stress/force-frequency relationship

The stress/force-frequency relationship of both specimens of donor hearts two and four was measured. Figure 3.2 demonstrates the measurement recording of specimen two from the second heart at 0 mN pre-stretch and an increase of the frequency (0.1 Hz to 2.0 Hz) every 300 s according to the testing protocol. A pronounced positive baseline shift starting at a frequency of about 1 Hz is remarkable in the plot which indicates viscoelastic behavior. This behavior could be observed in all tested specimens with slightly different starting points. Generally, the curve progression was nearly identical for all samples regardless of the pre-stretch.
Figure 3.3 shows a force-time diagram of the individual twitches at various frequencies of specimen one of the second heart at a pre-stretch of 100 mN. The figure indicates that

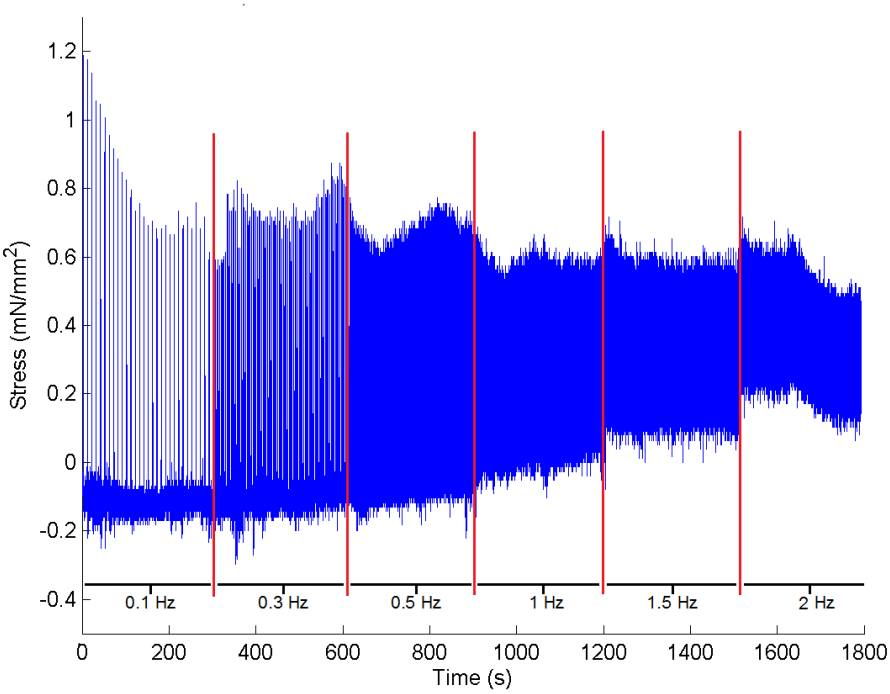

Figure 3.2: Measurement recording at 0 mN pre-stretch and an increase of the stimulation frequency every 300 s shown by red vertical lines; the pronounced baseline shift (starting at about 1 Hz) indicates a viscoelastic behavior (heart 2, specimen 2)

the twitch force and the twitch-time decrease with rising frequency. Moreover, the twitch-times correspond to the time of oscillation in the high frequency domain ($>$ 1 Hz) as can be seen in Fig. 3.3. The graphs in the frequency range from 1 to 2 Hz were cut off at their lowest points before next contraction.

Figure 3.4 shows the twitch stress behavior over the entire stimulation frequency range at different pre-stretches ((a) second heart; (b) fourth heart). The plot was generated by averaging the twitch peaks as mentioned in section 2.3.2. It is noticeable that the stresses of the first tested specimens are remarkably higher than those of the later tested ones. As already suggested in Fig. 3.3, an increase in stimulation frequency is accompanied by a decrease of the contraction force independent of the respective pre-stretch. Additionally, isometric peak developed stress gradually increases when the specimens are pre-stretched (except specimen two of the second heart) as can be seen in Fig. 3.4. The twitch stresses of the second heart (specimen one: 1.21 mN/mm^2 to 5.30 mN/mm^2, specimen two: 0.23 mN/mm^2 to 0.99 mN/mm^2) are distinctively higher than those of the fourth heart (specimen one: 0.31 mN/mm^2 to 0.52 mN/mm^2, specimen two: 0.19 mN/mm^2 to 0.41 mN/mm^2) - up to a factor of ten at equal pre-stretch. As can be recognized, some stress values at different stimulation frequencies are missing in the figure for following reasons: first, sometimes

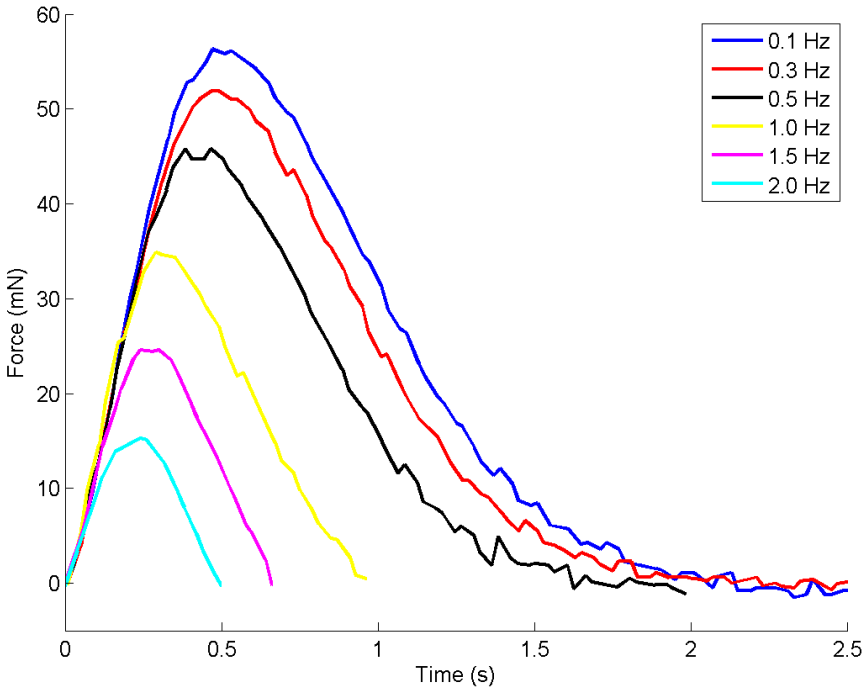

Figure 3.3: Single individual twitches at various frequencies at 100 mN pre-stretch (heart 2, specimen 1)

only every second stimulation led to contraction, particularly in the high frequency domain (specimen one of the fourth heart and specimen one of the second heart at 50 mN pre-stretch). Second, from a frequency of 2 Hz onwards and at a pre-stretch of 50 mN, it seems as if the cells of specimen two of the second heart had died. Third, the stress-frequency relationship of specimen one of the second heart at 0 mN pre-stretch indicates that the stimulation impulse arrived as early in the refractory period at the frequency transition from 0.5 Hz to 1.0 Hz as can be seen in Fig. 3.5. Only random noise could be measured until the stimulation frequency was reset to 0.1 Hz.

3.3 Twitch-time and time-to-peak

To evaluate the time behavior of the electrically induced twitch the twitch-time and the time-to-peak were analyzed. Figure 3.6 and 3.7 show the timing parameters of the second and fourth heart at various frequencies and pre-stretches. The colored bars represent the twitch-time, whereas the gray bars stand for the time-to-peak. Some bars are missing for the same reason as mentioned in section 3.2.

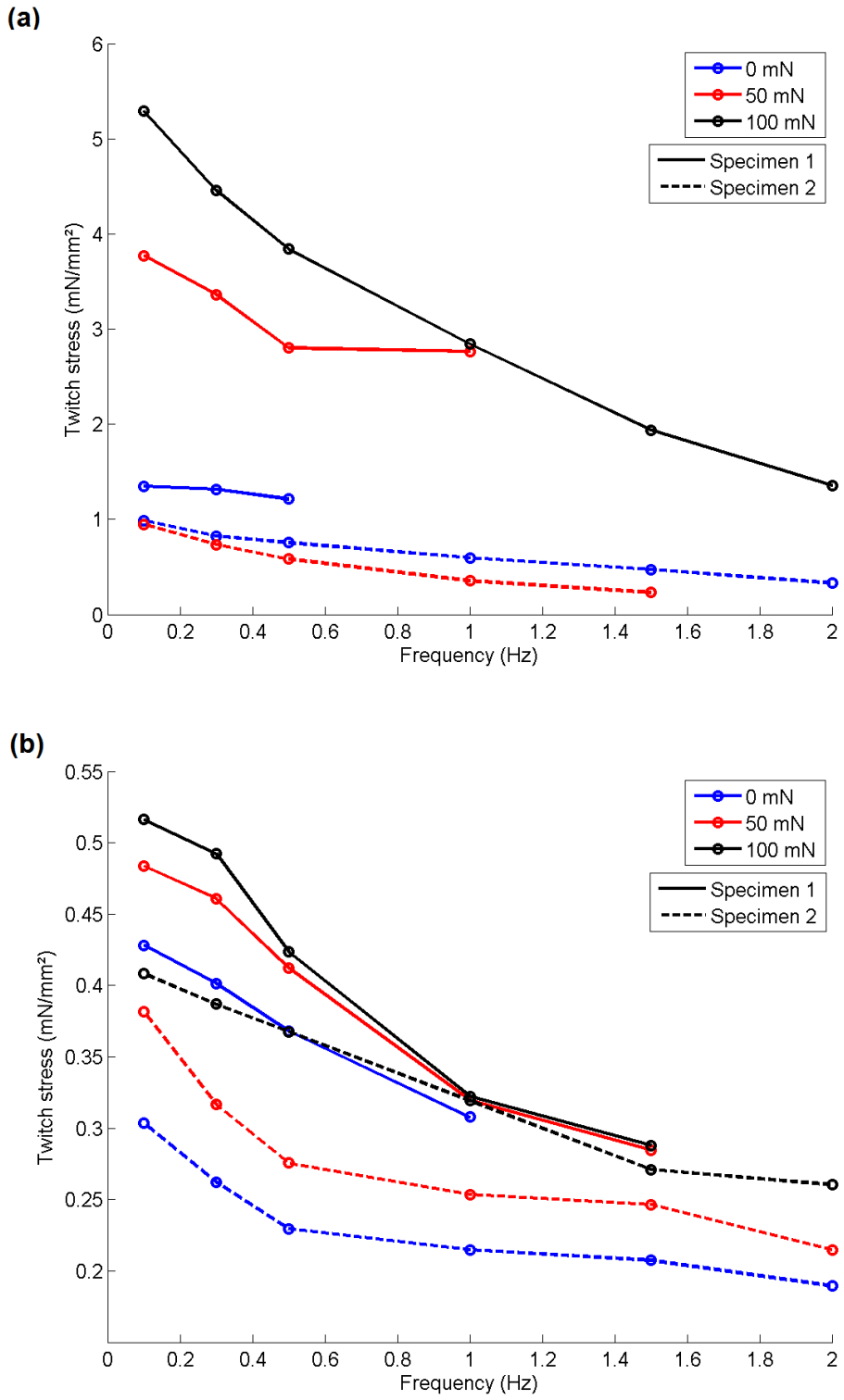

Figure 3.4: Twitch stress-frequency relationship about the total frequency range at various pre-stretches: (a) heart 2; (b) heart 4

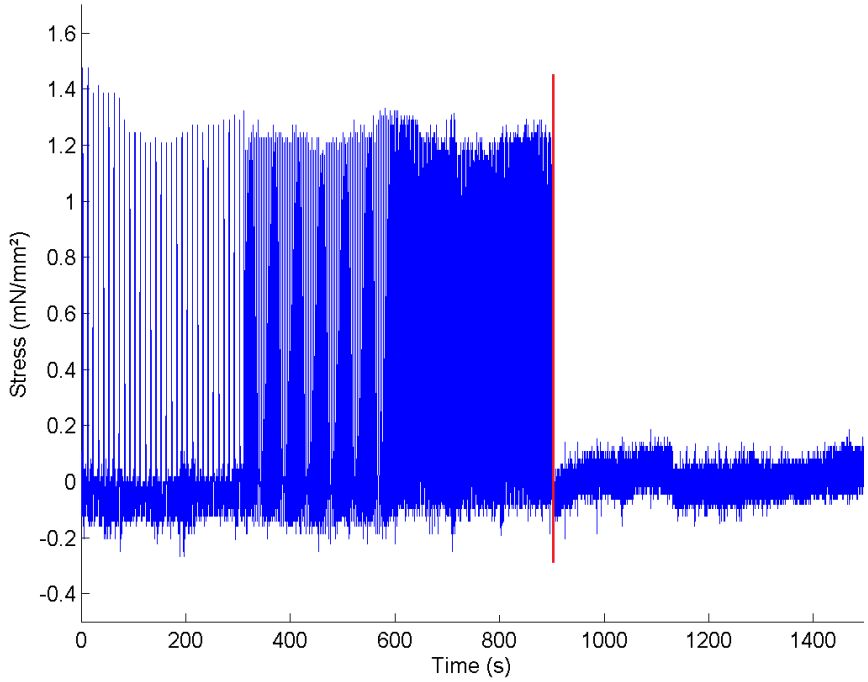

Figure 3.5: Refractory period at the frequency transition from 0.5 Hz to 1.0 Hz shown by the red vertical line (heart 2, specimen 1)

All of the timing parameters show a dependence on the stimulation frequency. The twitch-time as well as the time-to-peak decrease with increasing frequency (slightly pronounced for the time-to-peak of specimen two of the fourth heart). In contrast, no relationship of the timing parameters could be detected at various pre-stretches at the same frequency. The twitch-time and the time-to-peak are significantly higher at the second heart compared to the fourth heart. Furthermore, substantial differences in the timing parameters occur between the specimens of the second heart (higher time values at sample one compared to sample two). In contrast, this tendency is only slightly pronounced at the specimens of the fourth heart. Table 3.2 shows the timing parameters of the second and fourth heart respectively for both specimens.

Table 3.2: Timing parameters of the second and fourth heart

	Specimen 1		Specimen 2	
	Twitch-time (s)	Time-to-peak (s)	Twitch-time (s)	Time-to-peak (s)
Heart 2	1.50 ± 0.52	0.50 ± 0.16	1.08 ± 0.37	0.32 ± 0.11
Heart 4	0.72 ± 0.09	0.27 ± 0.03	0.67 ± 0.09	0.25 ± 0.07

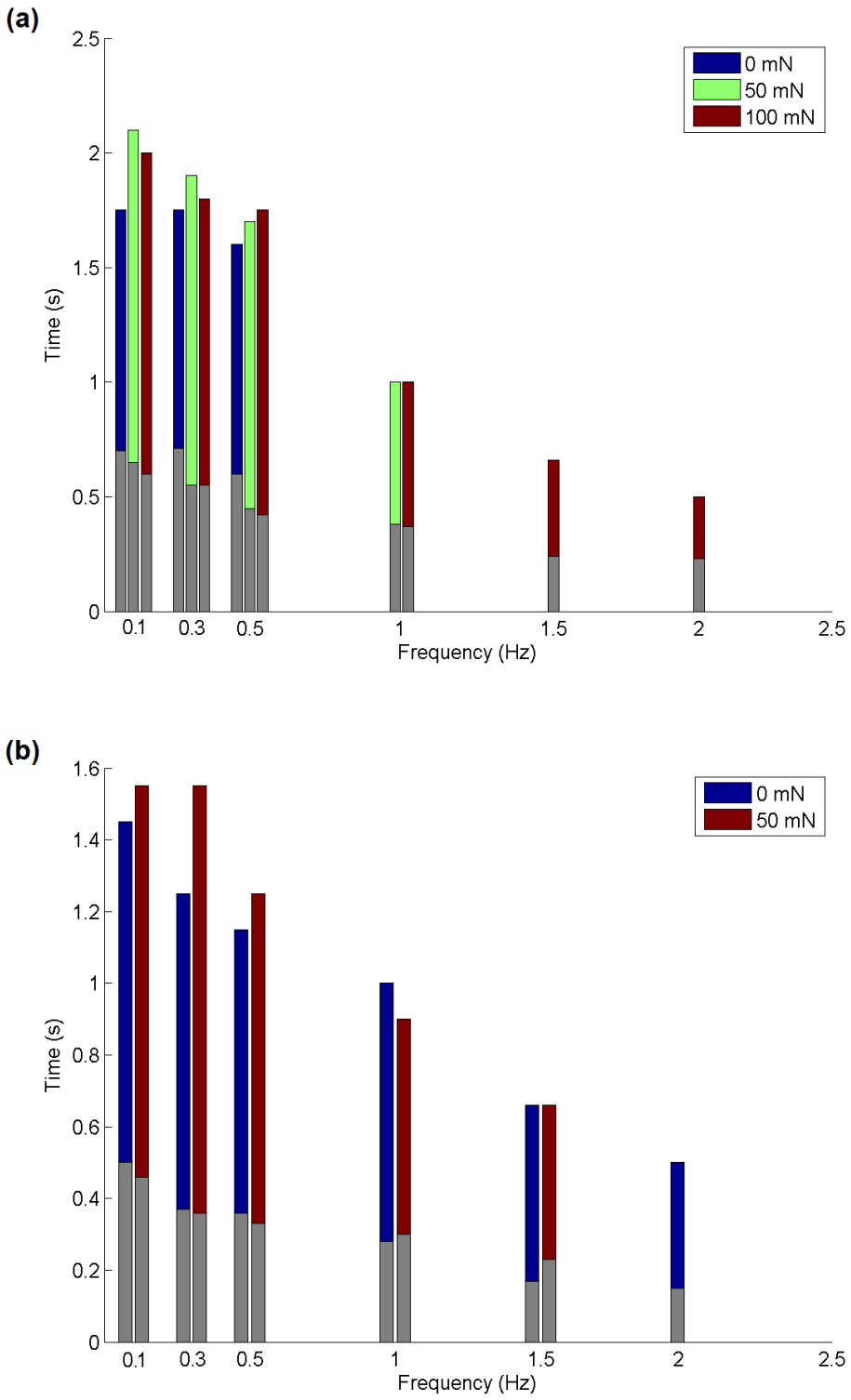

Figure 3.6: Twitch-time (colored bars) and time-to-peak (gray bars) of the second heart: (a) specimen 1; (b) specimen 2

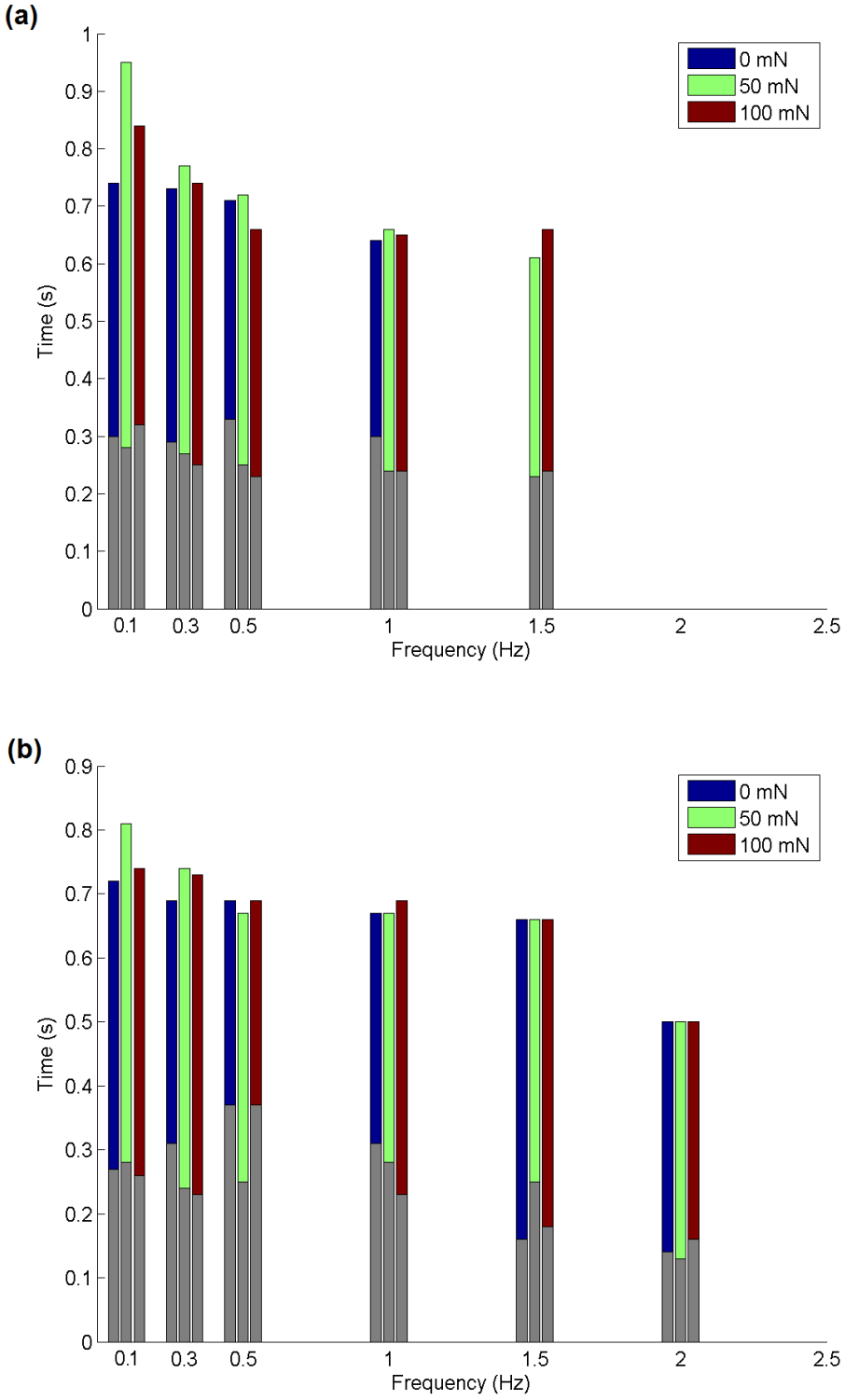

Figure 3.7: Twitch-time (colored bars) and time-to-peak (gray bars) of the fourth heart: (a) specimen 1; (b) specimen 2

The time-to-peak in dependence on the total twitch-time can be seen in Fig. 3.8. The red lines represent the standard deviation. It is noticeable that approximately only one third of the twitch-time is needed to reach the peak (second heart: 32.2 $\pm$ 5.7 %, fourth heart: 37.0 $\pm$ 7.1 %, second and fourth heart: 35.0 $\pm$ 6.9 %).

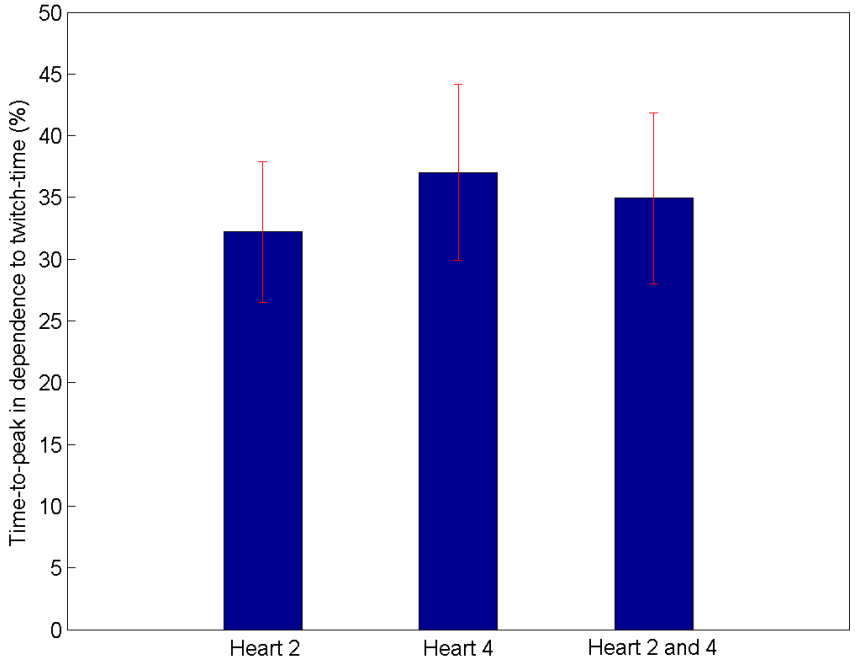

Figure 3.8: Time-to-peak in dependence on the twitch-time; the red lines represent the standard deviation

3.4 Control experiments

Figure 3.9 shows the conducted control experiments of specimen one of the second heart. In Fig. 3.9(a) the pulse width is changed from the standard 5 ms to 2.5 ms after 300 s of stimulation (demonstrated by the red vertical line). The variation of the stimulation voltage from the 'normal' voltage to a 50% increased stimulation voltage (in this particular case from 4.8 V to 7.2 V) after 300 s (demonstrated by the red line) can be seen in Fig. 3.9(b). In both cases, no noticeable changes in the curve progression, particularly in the twitch stress/force, could be detected for all performed control experiments.
Further, the bipolar Pt-micro-electrode was placed in the nutrient solution without direct contact to the specimen to see whether the myocardium would contract. A measurement

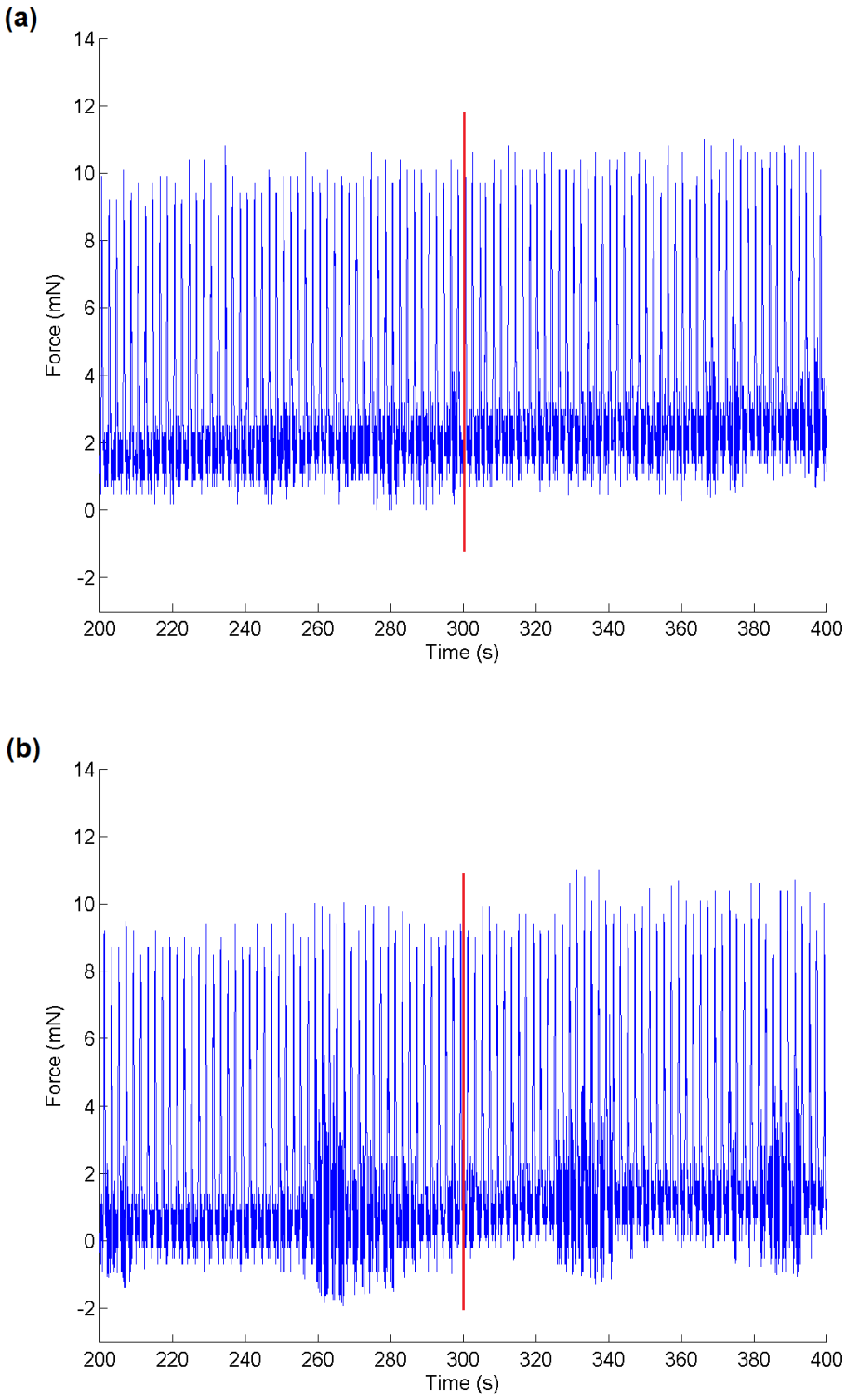

Figure 3.9: Conducted control experiments (heart 2, specimen 1): (a) alteration of the pulse width; (b) alteration of the stimulation voltage demonstrated after 300 s of stimulation by a red vertical line

recording of specimen one of the second heart is shown in Fig. 3.10 (stimulation parameters: frequency of 0.5 Hz and pulse width of 5 ms). As can be seen only noise was measured. The two distinctive peaks in the plot resulted from movements in the laboratory.

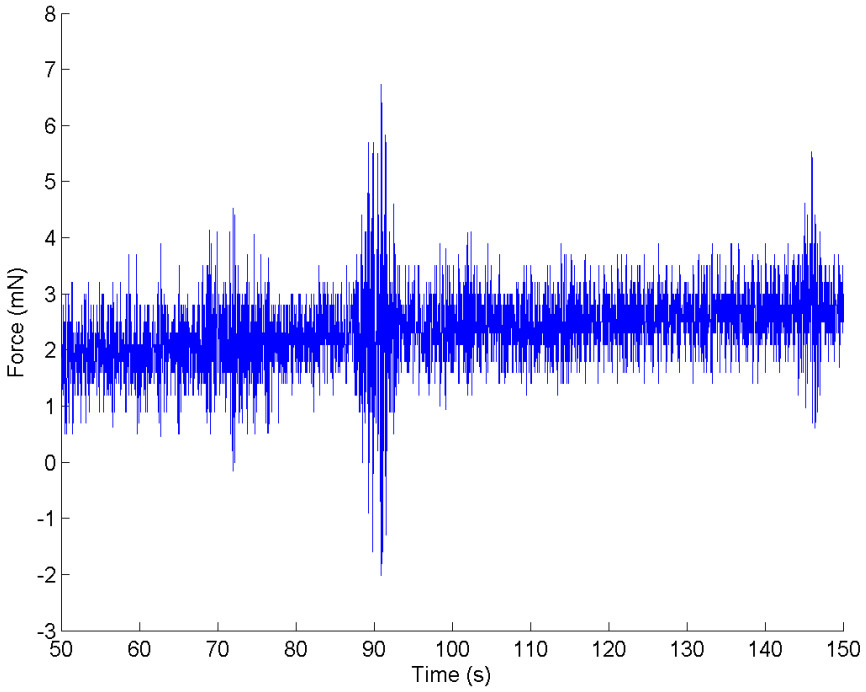

Figure 3.10: Measurement recording without direct contact of the electrode to the specimen (heart 2, specimen 1); only noise was measured; the two distinctive peaks resulted from movements in the laboratory

3.5 Strain data

The strain was exclusively measured for specimen two of the fourth heart. Figure 3.11 shows the two-dimensional strain at a pre-stretch of 100 mN and stimulation frequency of 0.5 Hz. In the left part of the figure the strain in x-direction (marker displacement in x-direction) is shown by color-plots, whereas in the right part the strain in y-direction (marker displacement in y-direction) can be seen. The recording times of the strain pictures from top to bottom are as follows: before stimulation, 0.19 s after stimulation impulse (maximum average strain value in y-direction), 0.45 s after stimulation impulse (maximum average strain value in x-direction), 0.9 s after stimulation impulse (specimen should be total

relaxed). Figure 3.11 indicates the strain is zero before stimulation, rises until the maximum is reached and decreases after contraction (relaxation). As can be seen, the displacement, and therefore the strain, is significantly higher in *y*- ($\varepsilon \leq 0.03$) than in *x*-direction ($\varepsilon \leq 0.01$). Every recorded image series of the fourth heart shows this tendency, independent of the stimulation frequency and pre-stretch. Furthermore, the two-dimensional strain exhibits a rather inhomogeneous distribution especially in *y*-direction. Badly tracked markers were deleted. Therefore the color plots do not show the full grid pixel dimensions as can be seen in the figure.
Figure 3.12 shows the average strain values of specimen two of the fourth heart in *y*-direction at a stimulation frequency of 0.5 Hz and 100 mN pre-stretch over an image series of 40 pictures (corresponds to a time period of 1 s). The average strain was calculated as mentioned in section 2.3.2. As can be seen, the average strain had been zero before the stimulation impulse arrived (image number 4). It then increased until peak was reached after the impulse and decreased again after contraction. Every average strain plot both in *x*- and in *y*-direction independent of the stimulation frequency and pre-stretch showed this behavior.
The characteristics of the peak average strain values (maximum value in Fig. 3.12) in *x*- and *y*-direction at different pre-stretches and stimulation frequencies of specimen two of the fourth heart can be seen in Fig. 3.13. The peak average strain values are distinctively higher in *y*- than in *x*-direction, as has already been recognized at the previously illustrated two-dimensional strain plots. The arithmetic mean is 0.0040 ± 0.0010 in *y*-direction and 0.0014 ± 0.0006 in *x*-direction over all frequencies and pre-stretches. Table 3.3 shows the mean values of the peak average strains in both directions grouped by pre-stretch. A correlation of the strain with the frequency could not be found.

Table 3.3: Arithmetic means of the peak average strains in *x*- and *y*-direction (heart 4, specimen 2)

Pre-stretch	Peak average strain in *x*-direction	Peak average strain in *y*-direction
0 mN	0.0020 ± 0.0004	0.0035 ± 0.0011
50 mN	0.0014 ± 0.0006	0.0049 ± 0.0006
100 mN	0.0009 ± 0.0003	0.0036 ± 0.0007

Figure 3.14 shows the strain time-to-peak at various pre-stretches and frequencies of specimen two of the fourth heart. Colored bars represent the time-to-peak in *x*-direction, whereas the gray bars stand for the *y*-direction. It seems as if, the strain time-to-peak is tendentiously higher in *x*- (0.45 ± 0.17 s) than in *y*-direction (0.26 ± 0.04 s). Further, the variation of the time parameter is smaller in *y*-direction compared to the *x*-direction.

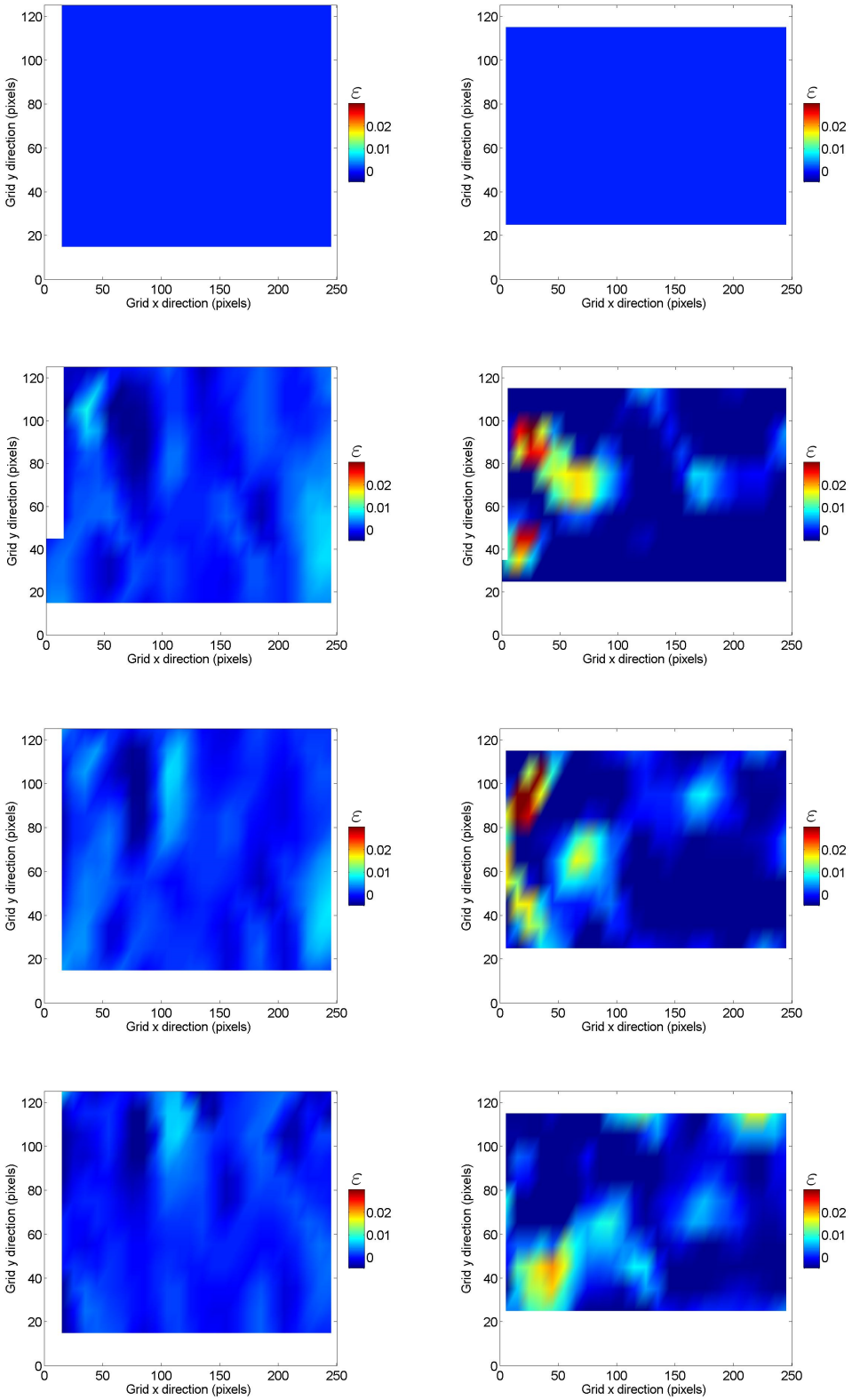

Figure 3.11: Two-dimensional strain in *x*- (left-hand side) and *y*-direction (right-hand side) at 100 mN pre-stretch and at a frequency of 0.5 Hz (heart 4, specimen 2); from top to bottom: before, 0.19 s after, 0.45 s after, and 0.90 s after stimulation

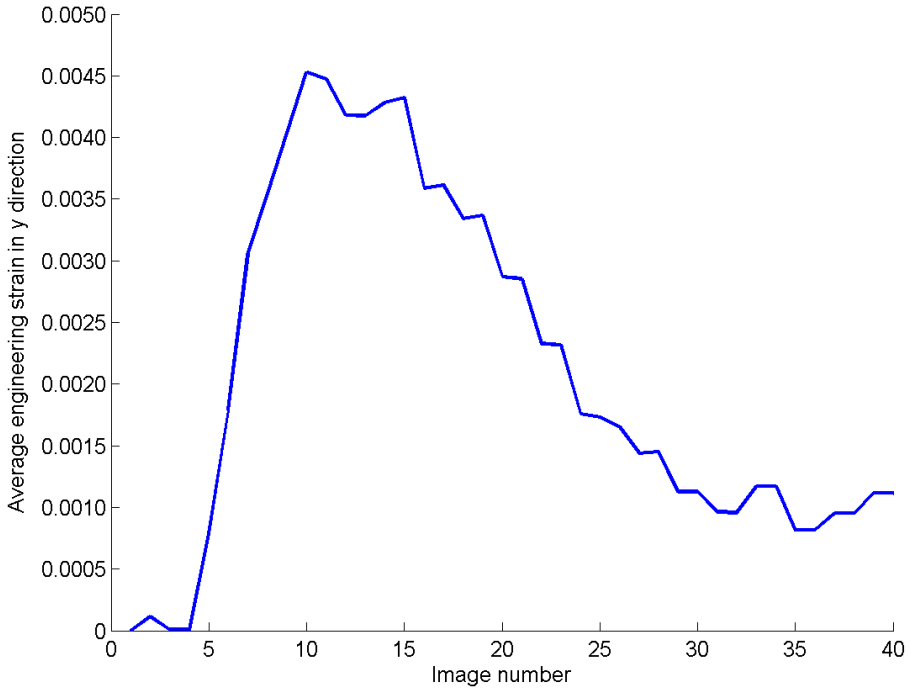

Figure 3.12: Average strain in y-direction at 0.5 Hz and 100 mN pre-stretch (heart 4, specimen 2); every average strain plot independent of the stimulation frequency and pre-stretch showed this behavior

3.6 Histology

To determine the fiber direction of the myocardium, histological studies were performed on the tested specimens of the second and fourth heart. Figure 3.15 shows representative histological images. The top row represents the H&E stain of specimen one of the second heart at a magnification of 5× (Fig. 3.15(a)) and 20× (Fig. 3.15(b)). Predominantly, muscle fibers were orientated longitudinally (specimen two shows a similar fiber orientation).
The histology of specimen two of the fourth heart (Fig. 3.15(c): magnification of 2.5×, Fig. 3.15(d): magnification of 20×) is shown at the bottom row of Fig. 3.15. In contrast to the samples of the second heart, muscle fibers of both specimens of the fourth heart were predominantly orientated transversally (more pronounced in sample two).

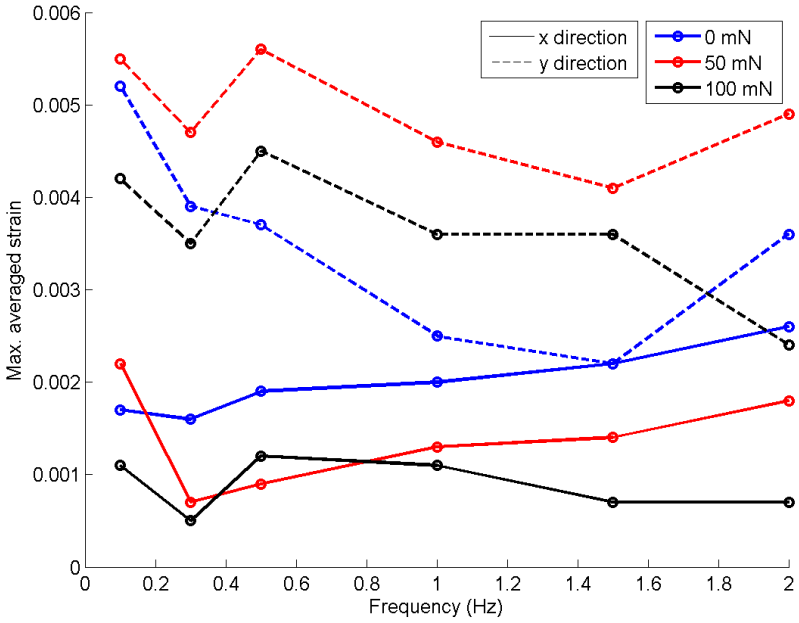

Figure 3.13: Characteristics of the peak average strain values (heart 4, specimen 2)

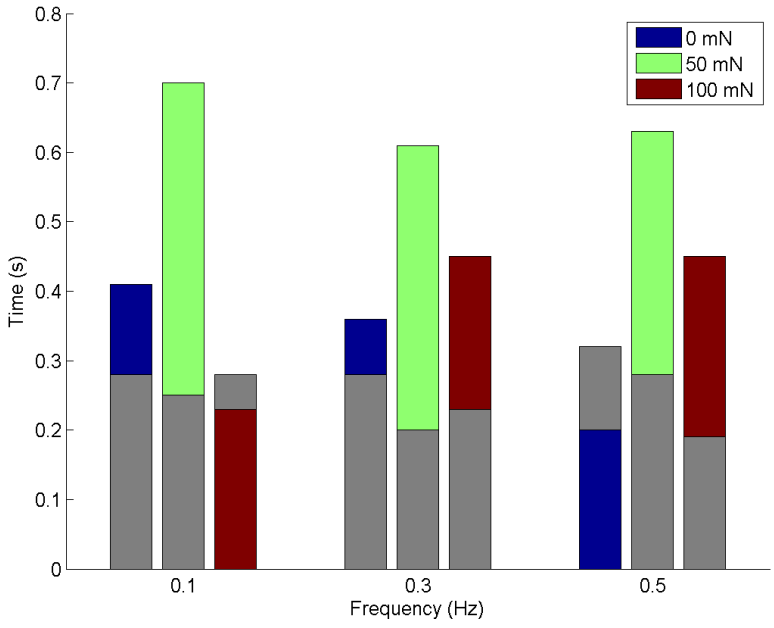

Figure 3.14: Strain time-to-peak at various pre-stretches and frequencies; colored bars: *x*-direction, gray bars: *y*-direction (heart 4, specimen 2)

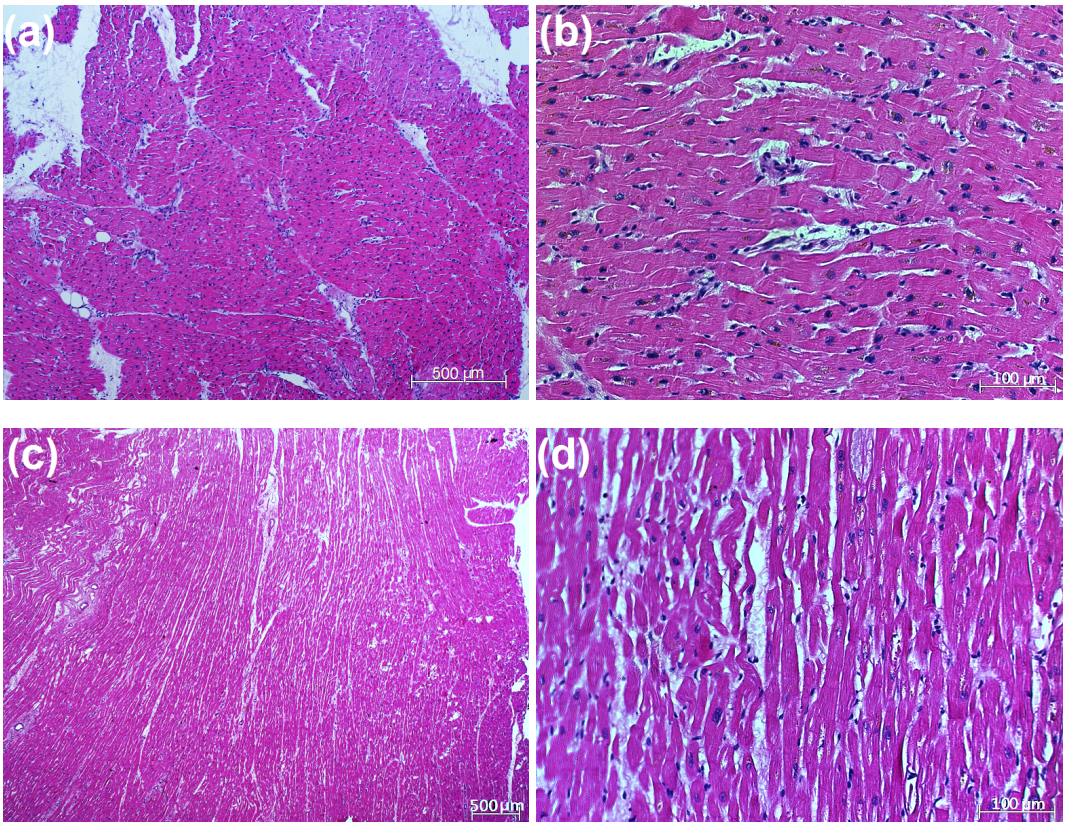

Figure 3.15: Representative histological images of the second and fourth heart specimens (dark-purple dots: cell nuclei; purple: cardioymyocytes; white: connective tissue): (a) heart 2, specimen 1, magnification 5×; (b) heart 2, specimen 1, magnification 20×; (c) heart 4, specimen 2, magnification 2.5×; (d) heart 4, specimen 2, magnification 20×; muscle fibers were predominantly orientated longitudinally at the second heart's specimens, in contrast to predominantly transversally oriented fibers at the fourth heart's specimens

4 Discussion

In this chapter, the experimental measured results are discussed. The focus is placed on the stress/force-frequency relationship and the strain data of the human myocardial specimens. In addition, the recordings of the threshold voltage and steady state, the twitch timing parameters, the conducted control experiments, and the histological report are discussed. The chapter concludes with occurring limitations, open problems and an outlook.

4.1 Threshold voltage and steady state

As can be seen at the pathological state in Table 2.1, the third myocardial tissue was affected by an inferior myocardial damage. This could explain why this tissue did not contract. Unfortunately, the specimens were not stored in formaldehyde to get a distinctive histological report whether the tested samples were healthy or not. According to Camelliti et al. (2011), 78 % of their obtained human heart slices (14 of 18 hearts) were viable.
The threshold voltage varied in a range of 4 V to 13 V. This is in relatively good agreement with reported values in literature. Camelliti et al. (2011) used a biphasic stimulation impulse for adult human heart slices with a threshold voltage of 1 V to 5 V. Ruf et al. (1998) related that a threshold voltage of 6 V by using an end-to-end square wave stimulation impulse for human atrial and ventricular myocardium. The threshold voltages in our study were slightly higher. The main reason could be that the specimens were placed in the testing solution and stimulated with the electrical impulse immediately after finishing the sample preparation process without a resting period to washout the cardioplegic solution and BDM by diffusion. Therefore, this could have led to an overestimation of the threshold voltage.
Except for specimen one of the second heart the steady state was reached within a range of 33.3 min to 43.3 min. Schwinger et al. (1993) reported that their human heart preparations were allowed to equilibrate for 90 min in a drug-free solution (1 Hz stimulation frequency) until complete mechanical stabilization was reached. An equilibration period of 60 min was chosen by Mulieri et al. (1992) for their human left ventricular muscle strip preparations. Ruf et al. (1998) reported a stabilisation time of 15 min for left ventricular myocardial slices. It seems as if the equilibration period in the literature tends to be longer than in this study. The reason presumably lies in a methodological cause: if there was no increase of twitch stresses after 5 min of stimulation, it was concluded that the steady state had been reached. This was done in order not to waste time and contrary to the above mentioned papers, in which a specified time period was chosen for equilibration. Interestingly, it took less time (8.3 min) until steady state was reached for specimen one of the

second heart. With a thickness of 1.5 mm this sample was thinner compared to the other specimens. This could have led to a faster out-streaming of the cardioplegic solution out of the tissue.
No data about the period of time until the first contraction occurred could be found in literature. Brandenburger et al. (2012) reported that they accepted human heart slices for contractility or electrophysiological investigations by electrical stimulation if a contractility could be registered within 30 min of experimentation. This scale is in good agreement with our measurement recordings (1500 s to 2000 s until the first contraction, except for specimen two of the second heart). This relatively long period of time may result from the process of rinsing the specimens from the BDM solution. This might also explain why it took more time until the later tested specimens contracted for the first time and reached the steady state. The longer the tissue stays in the cardioplegic solution, the more could diffuse into the myocardium.
Bussek et al. (2009) reported that the heart slices apparently fared well in the cardioplegic solution for up to 6 h. Reidemeister (1998) explained that human heart tissue is able to live up to 10 h in cardioplegia without considerable cellular damage. As can be seen in Table 3.2, the storage periods of the later used specimens were close to the above mentioned critical time range.
In addition, according to Camelliti et al. (2011) stable electrophysiological properties of human heart slices were maintained for up to 8 h from slice preparation in the Tyrode's nutrient solution. This time could always be adhered to (5 h maximal duration of observation).

4.2 Stress/force-frequency relationship

The cause of the significant baseline shift starting from 1 Hz to 1.5 Hz is the stimulation impulse arriving before the specimen is completely relaxed after the preceding impulse, indicating viscoelastic behavior as can be seen in Fig. 3.2. It confirms the assumption that the twitch-time corresponds to the time of oscillation in the high frequency domain (see Fig. 3.6 and 3.7). As human myocardial tissue shows viscoelastic behavior when tested for their passive elastic mechanical properties, the baseline shift was to be expected.
All tested specimens reveal a significant negative force-frequency relationship. This means that an increase of the stimulation frequency is accompanied by a reduction of force of contraction. Since the received hearts were classified as non-failing, a positive force-frequency relationship was expected. Several investigators demonstrated a positive relationship in non-failing human myocardial tissue slices. This important regulation mechanism was first reported by Henry Bowditch in 1871 (Bowditch (1871)). In these studies, the force of contraction increased with rising stimulation frequencies in non-failing myocardium but decreased in failing heart slices (Schwinger et al. (1993), Schwinger et al. (1997), Bavendiek et al. (1998), Holubarsch et al. (1998), Brixius et al. (2001), Janssen and Periasamy (2007)). Additionally, similar findings were reported *in vivo* (Feldman et al. (1988)). It is assumed that the negative force-frequency relationship in human my-

ocardium may result from an altered intracellular Ca^{2+}-handling. The exact reasons are yet unknown, but a decrease in the sarcoplasmatic reticulum calcium ATPase, an upregulation of the sodium-calcium exchanger and alterations of the protein-expression seem to be responsible for the inversed force-frequency relationship in heart failure (Schwinger et al. (1997), Bavendiek et al. (1998), Holubarsch et al. (1998)). Most obviously, insufficient oxygen and nutrient supply through to the core of the specimens may have led to the negative force-frequency relationship in this study. Schouten and ter Keurs (1986) stated that rat myocardial strips with diameters of more than 250 μm unavoidably suffers from a hypoxic core at room temperature and low stimulation frequency. Camelliti et al. (2011) claimed that adult human ventricular slices with a thickness of 250 μm to 350 μm are capable of exchanging oxygen at a rate sufficient for their metabolic requirement. If this ability is still existing in the presence of electrical stimulation, is yet unknown (Janssen and Periasamy (2007), Camelliti et al. (2011)). Nevertheless, our specimens are at least four times thicker compared to almost all human heart slice experiments in literature. This indicates that the limited oxygen and nutrient supply are the main cause for the negative force-frequency relationship in this study.

As can be seen in Fig. 3.4, the twitch stress/force increases by raising the pre-stretch of the specimens (except for specimen two of the second heart due to cell death). This basic experimental finding is clear and universally accepted. It is known as length-dependent activation and is one of the most important aspects to the well-known Frank-Starling mechanism, a critical part of normal cardiovascular function. Since the length-dependent activation was demonstrated in papillary muscle, trabeculae, and finally in each single myocardial cell, it is supposed that the mechanism exists on a multi-scale level. However, the functional basis of why this length-dependent activation happens remains unclear. To date, it seems evident that myofibrillar lattice spacing, titin-based effects, and cooperative activation are at least to some extent (Campbell (2011)).

One possible reason for the lower twitch stresses of the later tested specimens was reported by Brandenburger et al. (2012). They observed a significant and rapid rundown in force development of electrically stimulated human heart slices, even after the first day in cardioplegia (decrease of almost 90 % compared to immediately tested specimens) which indicates remodelling of the tissue due to mechanical inactivity. Evidence of myocyte necrosis caused by the alterations of the mechanical properties was not found. Mulieri et al. (1992) explained that there is no significant difference between peak isometric twitch stresses, whether the slices had been soaking in cardioplegic solution for one or ten hours. Compared to the above mentioned papers, the slices in this study were remarkably thicker, indicating that limited oxygen and nutrient supply also play a crucial role in the decreasing stress values of the later tested samples.

The different fiber orientation seems to be the main cause for the high variation of the twitch stresses between the specimens of the second and fourth heart (predominantly, samples of the second heart were oriented longitudinally, whereas specimens of the fourth heart were oriented transversally). Generally, the developed twitch stresses appear to be low in this study compared to reported values in literature. Schwinger et al. (1993) reported peak

twitch stresses of 4.6 mN/mm^2 vs. 3.5 mN/mm^2 (0.5 Hz vs. 2.0 Hz) in failing papillary muscle strips (cross-sectional area < 0.60 mm^2) from human left ventricular myocardium and of 4.0 mN/mm^2 vs. 7.3 mN/mm^2 in non-failing specimens. The measured values of specimen one of the second heart at 100 mN pre-stretch (3.84 mN/mm^2 vs. 1.36 mN/mm^2) are in good agreement with the failing data in the above mentioned paper. Brandenburger et al. (2012) reported maximum twitch contractions in freshly prepared failing endocardial human slices (thickness of 300 μm, stimulation frequency of 1 Hz) of 3.06 mN/mm^2. After one day in culture the twitch stress decreased to 0.35 mN/mm^2. Isometric twitch stresses of 22.8 mN/mm^2 in non-failing and 11.9 mN/mm^2 in failing human left ventricular tissue at a stimulation frequency of 1.2 Hz and a specimen cross-sectional area of less than 0.50 mm^2 were observed by Mulieri et al. (1992). Brixius et al. (2001) listed following electrically induced data: stress values of 11.3 mN/mm^2 vs. 19.9 mN/mm^2 (0.5 Hz vs. 2.0 Hz) in non-failing and of 12.1 mN/mm^2 vs. 7.1 mN/mm^2 in failing left ventricular papillary muscle strips (thickness of approximately 200 μm). In all of the above mentioned papers, the slices were cut parallel to their muscle cell orientation and were pre-stretched until the maximum twitch force was reached. For this reason, and because of essentially thinner specimens (better nutrient and oxygen supply), it seems reasonable that the twitch stresses in literature were higher under almost similar test conditions compared to the data in this study (range from 0.19 mN/mm^2 to 5.30 mN/mm^2).

4.3 Twitch-time and time-to-peak

The twitch-time and the time-to-peak decreased with increasing stimulation frequency, as can be seen in Fig. 3.6 and 3.7. This experimental finding is generally accepted (Sonnenblick et al. (1965), Schwinger et al. (1993)). Mulieri et al. (1992) reported that all of the timing parameters have a statistically significant dependence on the frequency in both failing and non-failing human myocardium. Janssen and Periasamy (2007) reported that the kinetics of contraction and relaxation is accelerated in human heart tissue by an increased stimulation frequency. The physiological reason for this is obvious. Filling, and thus cardiac output, is seriously affected if the heart does not relax in timely fashion before the next contraction is initiated. The frequency dependent acceleration of relaxation (FDAR) occurs at a cellular level. Investigations have focused on similar pathways responsible for the force-frequency relationship. Janssen and Periasamy (2007) found that not only the faster intracellular calcium decline, but also the myofilament responsiveness might play a critical role in the FDAR.
The twitch-time and the time-to-peak were higher in the specimens of the second heart compared to those of the fourth heart. In addition, timing parameters of samples of the second heart showed substantial differences. In both cases, the stress/force values of contraction differed remarkably. Therefore, it seems as if the timing parameters strongly depend on the developed twitch stresses, higher stress/force values lead to higher timing parameters. The same experimental finding was observed by Schwinger et al. (1997).
The timing parameters in this study are in relatively good agreement with published values

in literature. Sonnenblick et al. (1965) reported an averaged time-to-peak of 0.88 s at a frequency of 6 contractions per minute and 0.46 s at a stimulation frequency of 50 beats per minute in failing human left ventricular papillary segments. A twitch-time of 0.64 s and a time-to-peak of 0.16 s in non-failing (failing values: 0.67 s vs. 0.17 s) left ventricular myocardium were measured by Mulieri et al. (1992). Schwinger et al. (1997) related that the time-to-peak and the time to 95% tension decay in human papillary muscle strips were diminished significantly at 2 Hz compared with 0.5 Hz in non-failing (0.17 s vs. 0.21 s and 0.24 s vs. 0.43 s) and failing (0.19 s vs. 0.23 s and 0.27 s vs. 0.48 s) samples.
It only took approximately a third of the twitch-time until the maximum stress was reached. This means that the contraction of the myocardium takes less time than the relaxation. A similar value (time-to-peak in dependence on the total twitch-time of 25 %) was mentioned by Mulieri et al. (1992).

4.4 Control experiments

As anticipated, no noticeable variations in the curve progression, specifically in the twitch stress/force values, could be detected by changing the pulse width and the stimulation voltage. This is due to a peculiarity of the heart muscle which distinguishes it from the skeletal muscle. While the contraction of the skeletal muscle increases with increasing strength of the stimulus, the all-or-none phenomenon is applied to the heart. This means that a stimulation impulse produces a contraction or fails to do so corresponding to its strength. If this strength is high enough, the heart muscle produces the greatest contraction that can be produced by the myocardium at this deformation state.
As expected, the specimens did not contract without direct contact of the Pt-micro-electrode. In bipolar electrodes, anode and cathode are arranged so closely to each other that the current density, required to initiate an action potential and subsequently a contraction, is only high enough between the poles. Monopolar electrodes, on the other hand, are characterized by a large-scale electrical current flow which might be able to initiate a contraction without direct contact of the poles with the tissue. However, bipolar electrodes were used in every scientific paper, dealing with electrical stimulation of human myocardial tissue.

4.5 Strain data

The two-dimensional strain of human myocardial slices was measured for the first time, according to the knowledge of the author. Unfortunately, it was only measured for one particular specimen. Therefore, objective conclusions are difficult to draw. Notwithstanding, certain trends could be found.
Independent of the stimulation frequency and the pre-stretch, the two-dimensional strain was higher in y- than in x-direction. The reason for this is obvious: the muscle fibers of the tested specimen were predominantly oriented in the y-direction. In addition, the strain distribution was inhomogeneous with high local peak areas particularly in the y-direction.

It should be mentioned that this local peaks occurred not only in the vicinity of the Pt-micro-electrode. Hu et al. (2003) stated that the non-failing heart has a smoother strain distribution than the failing heart by *in vivo* strain estimation of left and right ventricles from MRI images. Inspecting the individual two-dimensional strain plots from one particular image series it can be noticed that the subjectively highest strain plot coincided well with the peak of the corresponding average strain plot.
The strain was in a range of $\varepsilon \leq 0.01$ in *x*-direction and of $\varepsilon \leq 0.03$ in *y*-direction which coincides with a central segment shortening of ≤ 1 to 3 %. Holubarsch et al. (1998) reported a one-dimensional central segment shortening in electrically stimulated thin human left ventricle papillary muscle preparations (cross-sectional area of ≤ 0.43 mm^2) of 0.5 % of the whole muscle length. This value is in good agreement with the *x*-direction strain in this study. A fractional shortening of about 8 % in failing and non-failing ventricular cardiomyocytes at a stimulation frequency of 0.5 Hz was described by Brixius et al. (2001). In addition, they observed a high frequency dependence of the shortening. It is, of course, questionable to what extent strains from individual cells can be compared to tissue slices.
As expected, the average strain plots in both *x*- and *y*-direction always showed the same characteristics: the strain was zero before stimulation, rose until peak was reached after stimulation and decreased afterwards.
Contrary to the twitch stress behavior, no dependence of the frequency on the peak average strain characteristic (see Fig. 3.13) could be found. Furthermore, it seems that the peak average strain in *x*-direction decreased with increasing pre-stretch (in contrast, no dependence could be found in *y*-direction). One possible reason might be the specimen had already been stretched too much at a pre-stretch of 100 mN to determine any feasible deformations on the surface. The isotonic experimental setup is an alternative approach to study the strain. In isotonic experiments, one end of the tissue slice is fixed while the other end is free to move as the muscle contracts. Holubarsch et al. (1998) reported a one-dimensional central shortening in isometric experiments which was less than 5 % of maximal shortening in isotonic contraction experiments.
As expected, the peak average strain values were higher in *y*-direction (ε = 0.0040 $\pm$ 0.0010) than in *x*-direction (ε = 0.0014 $\pm$ 0.0006). Compared to local peak areas in the two-dimensional strain plots, the above mentioned peak values were underestimated due to a linear regression fit (see Fig. 2.14).
Although the strain in *x*-direction is smaller than in *y*-direction, in most cases, the strain peak was reached earlier in *y*-direction. Therefore, the behavior of strain time-to-peak differs from the stress' behavior in which higher twitch stress/force values lead to higher timing parameters. In contrast to the stress time-to-peak, no dependence of the frequency on the strain time-to-peak could be found. The stress time-to-peak values of specimen two of the fourth heart agree well with the strain time-to-peak values in *y*-direction. The same behavior was reported by Krueger and Pollack (1975). They noted that the maximal sarcomere length shortening during contraction occurred near the time of peak twitch force in electrically stimulated thin rat papillary muscles from the right ventricles.

4.6 Histology

Basically, the histological report indicates a healthy state of the myocardium with partially enlarged cell nuclei (represented by dark-purple dots in Fig. 3.15). The cause of the enlarged cell nuclei may have many reasons from hypertension to serious heart failure. Unfortunately, H&E histology is not able to detect cell damage that occurs during the experimental task, for example by oxygen and nutrient deficiency which would be of great interest.

4.7 Limitations

One of the biggest problems during the experimental task was the cutting process. Uniform specimens were essential to perform the experiments. It was, however, demanding to cut thin and uniform slices with a bulky universal cutter from the very soft consistency of the myocardium. Additionally, the thin myocardial wall showed no homogeneous structure.
The heating coil and the gas supply could only be switched on during experimental breaks. Both led to such a high noise level that the measurement recordings were considerably overlain. Nevertheless, the temperature could be kept in a range of 37°C $\pm$ 1°C.
The uniaxial tensile testing machine is very sensitive to external environmental conditions. A mere step or a closing door in the laboratory could affect the measurements.
The slice thickness seems to be the biggest limitation leading to negative stress/force-frequency relationship. Obviously, sufficient nutrient and oxygen supply through to the core could not be maintained. Slice thickness and cross-sectional area (1.5 mm to 2.2 mm respectively 11.25 mm^2 to 17.60 mm^2) were remarkably higher in this study compared to other human myocardial slice experiments in literature. Mulieri et al. (1989) reported that the cross sections of cardiac specimens should be less than 0.59 mm^2 for adequate oxygenation at physiological temperature and stimulation frequency.
It was intended to cut slices parallel to their muscle fiber direction. It was, however, not possible to consider the fiber orientation due to the small size of the received tissue. This, in combination with the fact that the specimens were not pre-stretched, the condition in which they would have had their maximum twitch stress, probably led to the lower twitch values compared to reported stresses in literature.
It can not be ruled out that the instant adhesive, especially at the ends of the specimens and spraying the samples with black color had negative effects. In addition, the dissection injury on the surface of the slices might have negatively influenced the results, although the use of 2,3-butanedione monoxime should have kept those injuries as low as possible (Mulieri et al. (1989)).
Since Tyrode's is the standard solution, the possibility of DMEM influencing the results measured cannot be ruled out.
Due to a lack of comparative values, the extent to which Digital Image Correlation is suitable for calculating strain from the pixel displacement of an image series is unclear.

4.8 Improvements and outlook

Thinner human myocardial slices cut in muscle fiber direction, e.g., by using vibratome sectioning, should be further tested to get more representative findings in order to extend the material parameters of the Institute of Biomechanics FEM heart model by active mechanical properties. Additionally, the pre-stretch of the specimens should be chosen more physiologically to approach a pressure of 15 kPa, similar to the pressure in the human left ventricle *in vivo* (in this study 5.68 kPa to 8.89 kPa because a specimen thickness of about 1 mm was assumed - thickness and width measurement were made after the activation tests in order to guarantee best survival conditions).
In further investigations, image series should also be recorded in an isotonic experimental setup in which the specimen is free to move as the muscle contracts to measure the two-dimensional strain.

5 Conclusion

An experimental setup based on an uniaxial tensile testing machine, which is able to measure the twitch-stresses/forces and the one- and two-dimensional strains of electrically activated human ventricular myocardial slices in the bradycardial, physiological, and tachycardial frequency range, could be established.
The twitch-stress revealed an interesting behavior: although the received hearts were classified as non-failing (confirmed by histological examination) a negative stress/force-frequency relationship was observed indicating failing tissue. Additionally, it was shown that the length-dependent activation, one of the most important aspects to the Frank-Starling mechanism, is still existing in human heart slices (higher twitch-stresses at higher pre-stretches).
For the first time, according to the knowledge of the author, the two-dimensional strain on the surface of the specimen was measured. The strain characteristics of a single contraction cycle showed the expected behavior which might be an indicator of plausible data. Although measurement records showed clear tendencies, making further statements is difficult because only one specimen's strain field was measured and no comparative values are available in the literature.
For both stress and strain data, timing-parameters were acquired to gather information on the time course of contraction.
The experimental setup can be used to study the reaction of failing human left ventricular myocardial slices to drug treatment and can provide a suitable preclinical model for drug safety screening. The reversal of the negative stress/force-frequency relationship is of course of considerable importance in heart failure therapy and thus, represents an promising market for the pharmaceutical industry.

Bibliography

U. Bavendiek, K. Brixius, G. Münch, C. Zobel, J. Müller-Ehmsen and R. H. Schwinger. *Effect of inotropic interventions on the force-frequency relation in the human heart*. Basic Res Cardiol, 93: Suppl. 1, 76–85, 1998.

H. P. Bowditch. *Über die Eigentümlichkeiten der Reizbarkeit, welche die Muskelfasern des Herzens zeigen*. Ber Sachs Ges Akad Wiss, 23: 652–689, 1871.

M. Brandenburger, J. Wenzel, R. Bogdan, D. Richardt, F. Nguemo, M. Reppel, J. Hescheler, H. Terlau and A. Dendorfer. *Organotypic slice culture from human adult ventricular myocardium*. Cardiovascular Research, 93: 50–59, 2012.

K. Brixius, S. Hoischen, H. Reuter K. Lasek and R. H. Schwinger. *Force/Shortening-frequency relationship in multicellular muscle strips and single cardiomyocytes of human failing and nonfailing hearts*. Journal of Cardiac Failure, Vol. 7 No. 4, 2001.

A. Bussek, M. Schmidt, J. Bauriedl, U. Ravens, E. Wettwer and H. Lohmann. *Cardiac tissue slices with prolonged survival for in vitro drug safety screening*. Journal of Pharmacological and Toxicological Methods, 66: 145–151, 2012.

A. Bussek, E. Wettwer, T. Christ, H. Lohmann, P. Camelliti and U. Ravens. *Tissue slices from adult mammalian hearts as a model for pharmacological drug testing*. Cellular Physiology and Biochemistry, 24: 527–536, 2009.

P. Camelliti, S. A. Al-Saud, R. T. Smolenski, S. Al-Ayoubi, A. Bussek, E. Wettwer, N. R. Banner, C. T. Bowles, M. H. Yacoub and C. M. Terracciano. *Adult human heart slices are a multicellular system suitable for electrophysiological and pharmacological studies*. Journal of Molecular and Cellular Cardiology, 51: 390–398, 2011.

K. S. Campbell. *Impact of myocyte strain on cardiac myofilament activation*. Pflugers Arch, 462: 3–14, 2011.

Custodiol about. URL: $http://www.custodiol.com/about-custodiol.php$

Custodiol data sheet. URL: $http://www.pharmazie.com/graphic/A/42/1-20642.pdf$

M. Endoh. *Force-frequency relationship in intact mammalian ventricular myocardium: physiological and pathophysiological relevance*. European Journal of Pharmacology, 500: 73–86, 2004.

J. Erhard, A. E. Daul and F. W. Eigler. *Organspende und Organkonservierung*. Deutsches Ärzteblatt 92, Heft 1/2 , 43–49, 1995.

M. D. Feldman, J. D. Alderman, J. M. Aroesty, H. D. Royal, J. J. Ferguson, R. M. Owen, W. Grossman and R. G. McKay. *Depression of systolic and diastolic myocardial reserve during atrial pacing tachycardia in patients with dilated cardiomyopathy*. J. Clin. Invest., 82: 1661–1669, 1988.

G. Hasenfuss, L. A. Mulieri, E. M. Blanchard, C. Holubarsch, B. J. Leavitt, F. Ittleman and N. R. Alpert. *Energetics of isometric force development in control and volume-overload human myocardium. Comparison with animal species*. Circulation Research, 68: 836–846, 1991.

M. A. Hassan, M. Hamdi and A. Noma. *The nonlinear elastic and viscoelastic passive properties of left ventricular papillary muscle of a Guinea pig heart*. Journal of the mechanical behavior of biomedical materials, 5: 99–109, 2012.

C. Hick and A. Hick. *Intensivkurs Physiologie*. Elsevier GmbH, München; Edition: 5, 2006.

Ch. Holubarsch, J. Lüdemann, S. Wiessner, Th. Ruf, H. Schulte-Baukloh, S. Schmidt-Schweda, B. Pieske, H. Posival and H. Just. *Shortening versus isometric contractions in isolated human failing and non-failing left ventricular myocardium: dependency of external work and force on muscle length, heart rate and inotropic stimulation*. Cardiovascular Research, 37: 46–57, 1998.

G. A. Holzapfel and M. Unterberger. *Lecture: 'Einführung in die Biomechanik - 450.009', Graz University of Technology*. Summer term 2010.

Z. Hu, D. Metaxas and L. Axel. *In vivo strain and stress estimation of the heart left and right ventricles from MRI images*. Medical Image Analysis, 7: 435–444, 2003.

P. M. L. Janssen and M. Periasamy. *Determinants of frequency-dependent contraction and relaxation of mammalian myocardium*. Journal of Molecular and Cellular Cardiology, 43: 523–531, 2007.

J. W. Krueger and G. H. Pollack. *Myocardial sarcomere dynamics during isometric contraction*. J. Physiol., 251: 627–643, 1975.

F. Moussavi-Harami, M. V. Razumova, A. W. Racca, Y. Cheng, A. Stempien-Otero and M. Regnier. *2-Deoxy adenosine triphosphate improves contraction in human end-stage heart failure*. Journal of Molecular and Cellular Cardiology, 79: 256–263, 2015.

L. A. Mulieri, G. Hasenfuss, F. Ittleman, E. M. Blanchard and N. R. Alpert. *Protection of human left ventricular myocardium from cutting injury with 2,3-butanedione monoxime*. Circulation Research, 65: 1441–1449, 1989.

L. A. Mulieri, G. Hasenfuss, B. Leavitt, P. D. Allen and N. R. Alpert. *Altered myocardial force-frequency relation in human heart failure*. Circulation, 85: 1743–1750, 1992.

N. Oezkaya and M. Nordin. *Fundamentals of biomechanics. Equilibrium, motion and deformation*. Springer, Berlin; Edition: 2. A., 1999.

N. S. Phatak, S. A. Maas, A. I. Veress, N. A. Pack, E. V. R. Di Bella and J. A. Weiss. *Strain measurement in the left ventricle during systole with deformable image registration*. Medical Image Analysis, 13: 354–361, 2009.

A. R. Pombinho, V. Laizé, D. M. Molha, S. M. P. Marques and M. L. Cancela. *Development of two bone-derived cell lines from the marine teleost Sparus aurata ; evidence for extracellular matrix mineralization and cell-type-specific expression of matrix Gla protein and osteocalcin*. Cell and Tissue Research, 315: 393–406, 2004.

W. Pschyrembel. *Hunnius klinisches und pharmazeutisches Wörterbuch, CD-ROM*. de Gruyter, Berlin; 2004.

J. C. Reidemeister. *Herz- und Lungentransplantationen. Thorakale Transplantationen: Stand und Ausblick*. Essener Unikate 10/1998, 54–61, 1998.

T. Ruf, H. Schulte-Baukloh, J. Lüdemann, H. Posival, F. Beyersdorf, H. Just and C. Holubarsch. *Alterations of cross-bridge kinetics in human atrial and ventricular myocardium*. Cardiovascular Research, 40: 580–590, 1998.

V. J. A. Schouten and H. E. D. J. ter Keurs. *The force-frequency relationship in rat myocardium. The influence of muscle dimensions*. Pflugers Arch, 407: 14–17, 1986.

R. H. Schwinger, M. Böhm, J. Müller-Ehmsen, R. Uhlmann, U. Schmidt, A. Stäblein, P. Uberfuhr, E. Kreuzer, B. Reichart and H. J. Eissner. *Effect of inotropic stimulation on the negative force-frequency relationship in the failing human heart*. Circulation, 88: 2267–2276, 1993.

R. H. Schwinger, K. Brixius, U. Bavendiek, S. Hoischen, J. Müller-Ehmsen, B. Bölck and E. Erdmann. *Effect of cyclopiazonic acid on the force-frequency relationship in human nonfailing myocardium*. The Journal of Pharmacology and Experimental Therapeutics, 283: 286–292, 1997.

H. A. Shiels, M. Vornanen and A. P. Farrell. *The force-frequency relationship in fish hearts - a review*. Comparative Biochemistry and Physiology, 132: 811–826, 2002.

S. D. Solomon. *Essential echocardiography: a practical guide with DVD*. Humana Press, Totowa, New Jersey; 2007.

G. Sommer, T. C. Gasser, P. Regitnig, M. Auer and G. A. Holzapfel. *Dissection properties of the human aortic media: an experimental study*. Journal of Biomechanical Engineering, 130: 021007, 2008.

G. Sommer, M. Kutschera, R. Kresnik, M. Schwarz, T. Eriksson, G. Plank and G. A. Holzapfel. *Lecture: 'Mechanical properties of passive human ventricular myocardium', Cardiology meeting, Medical University of Graz.* 2012.

E. H. Sonnenblick, E. Braunwald and A. G. Morrow. *The contractile properties of human heart muscle: studies on myocardial mechanics of surgically excised papillary muscles*. Journal of Clinical Investigation, Vol. 44, No. 6, 1965.

E. J. Speckmann and W. Wittkowski. *Bau und Funktion des menschlichen Körpers*. Elsevier GmbH, München; Edition: 20, 2004.

G. Ziemer and A. Haverich. *Herzchirurgie: Die Eingriffe am Herzen und an den herznahen Gefäßen*. Springer-Verlag, Berlin Heidelberg; Edition: 3, 2011.

Statutory Declaration

I declare that I have authored this Thesis independently, that I have not used other than the declared sources/resources, and that I have explicitly marked all material, which has been quoted by the relevant reference.

date

signature